

A MODEL FOR HOT-CARRIER INDUCED SUBSTRATE CURRENTS IN MOS TRANSISTORS

by

Syed Afjal Hossain

A Thesis

Submitted to the Department of Electrical and Electronic Engineering in
partial fulfilment of the requirements for the degree of

of

Master of Science in Electrical and Electronic Engineering

DEPARTMENT OF ELECTRICAL AND ELECTRONIC ENGINEERING,
BANGLADESHI UNIVERSITY OF ENGINEERING AND TECHNOLOGY.

DHAKA-1000, BANGLADESH.

JANUARY 07, 1997



#90718#

DECLARATION

I hereby declare that this thesis work has been done by me and it has not been submitted elsewhere for the award of any degree or diploma.

Countersigned

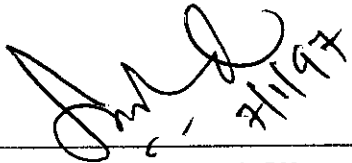
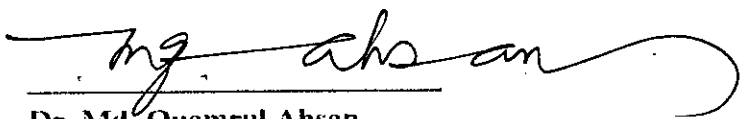
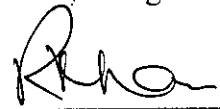
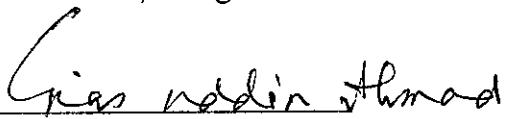
(Dr. Quazi Deen Mohd Khosru)

(Syed Afjal Hossain)

Syed Afjal Hossain

The thesis "A MODEL FOR HOT-CARRIER INDUCED SUBSTRATE CURRENTS IN MOS TRANSISTORS" submitted by Syed Afjal Hossain, Roll No. 921348P, Session 1990-91-92 to the Electrical and Electronic Engineering Department of BUET has been accepted as satisfactory for partial fulfillment of the requirements for the degree of Master of Science in Engineering (Electrical and Electronic).

BOARD OF EXAMINERS

1. 
Dr. Quazi Deen Mohd Khosru
Assistant Professor
Department of Electrical and
Electronic Engineering, BUET,
Dhaka-1000, Bangladesh.
Chairman
(Supervisor)
2. 
Dr. Md. Quamrul Ahsan
Professor and Head
Department of Electrical and
Electronic Engineering, BUET,
Dhaka-1000, Bangladesh.
Member
(Ex-officio)
3. 
Dr. M. Rezwan Khan
Professor
Department of Electrical and
Electronic Engineering, BUET,
Dhaka-1000, Bangladesh.
Member
4. 
Dr. Giasuddin Ahmad
Professor and Head
Department of Physics, BUET,
Dhaka-1000, Bangladesh.
Member
(External)

CONTENTS

| | |
|-----------------------|------|
| ACKNOWLEDGEMENT | iv |
| ABSTRACT..... | v |
| LIST OF SYMBOLS | vi |
| LIST OF FIGURES..... | viii |

1. INTRODUCTION

| | |
|---|----|
| 1.1 MOS transistors fundamentals..... | 1 |
| 1.2 Effect of substrate bias..... | 10 |
| 1.3 Additional features of short-channel MOSFET..... | 12 |
| 1.4 Avalanche breakdown and Hot-carrier effect..... | 13 |
| 1.5 Review of recent works on substrate current modeling of MOSFET..... | 16 |
| 1.6 Objective of the thesis..... | 18 |
| 1.7 Summary of the dissertation..... | 19 |

2. A MODEL FOR HOT-CARRIER INDUCED SUBSTRATE CURRENTS IN MOS TRANSISTORS

| | |
|--|----|
| 2.1 Introduction..... | 21 |
| 2.2.1 Current-voltage relation in MOS transistors..... | 23 |
| 2.2.2 Determination of drain saturation voltage..... | 26 |
| 2.3.1 Local-field model..... | 30 |
| 2.3.2 Nonlocal impact ionization model..... | 32 |
| 2.4 Analytical substrate current model..... | 38 |
| 2.5 Effects of substrate current | 40 |
| 2.5.1 Enhanced body effect..... | 40 |
| 2.5.2 Bipolar transistor action of MOSFET..... | 41 |
| 2.6 Conclusions..... | 43 |

3. MODEL IMPLEMENTATION AND RESULTS

| | |
|-----------------------------|----|
| 3.1 Introduction..... | 44 |
| 3.2 Results and discussions | |

| | |
|--|-----------|
| 3.2.1 Drain current characteristics..... | 46 |
| 3.2.2 Local-field model..... | 46 |
| 3.2.3 Non local impact ionization model..... | 53 |
| 3.2.4 Substrate current model..... | 56 |
| 3.2.5 Depletion width and the base emitter voltage | 60 |
| 3.3 Conclusions..... | 63 |
| 4. CONCLUSIONS | |
| 4.1 Conclusions..... | 64 |
| 4.2 Suggestions..... | 65 |
| APPENDIX -A | 66 |
| APPENDIX -B | 72 |
| REFERENCES..... | 74 |

ACKNOWLEDGEMENT

The author would like to express his sincere and heartiest gratitude to Dr. Qauzi Deen Mohd. Khosru, Assistant Professor of the Department of Electrical and Electronic Engineering, BUET, for his continued guidance, friendly supervision, encouragement, cooperation and valuable suggestions to complete this work.

The author wishes to express his heartiest thanks and regards to Prof. M. Rezwana Khan, Prof. M.A. Matin and Prof. Md. Quamrul Ahsan, Head of the Department of Electrical and Electronic Engineering, BUET, for support to complete this work.

Sincere thanks to all colleagues and friends for their cooperation. The author is grateful to his parents, brothers, bhavi and sister for their encouragement.

ABSTRACT

Hot-carrier induced degradation is one of the main concern in MOSFET's . One manifestation of the presence of such hot-carrier is the substrate current resulting from impact ionization of carriers in the high field region near the drain. The measurement of substrate current has become an important and widely used method for monitoring the presence of energetic carriers. For this reason, the substrate current itself has been used as a parameter in modeling device reliability. The impact ionization events generally occur near the drain where highly nonuniform electric field exists. The channel electrons experiencing rapid change of electric field do not reach their stationary state transport. The non-stationary transport of electrons could affect the impact ionization . It has been found that the established local-field model can introduce an artificially high and misleading degree of sensitivity in substrate current. But the quantitative argument of the non-local impact ionization in MOSFET's is still lacking. In this work, a non-local impact ionization model applicable for the drain region is proposed where electric field increases exponentially. From the non-local impact ionization model, a new analytical model for substrate current is developed which explained the experimental data quite well.

LIST OF SYMBOLS

| Symbol | Unit | Description |
|-------------|-----------|---|
| V_{DB} | Volts | Drain bulk voltage |
| V_{GB} | Volts | Gate bulk voltage |
| V_{SB} | Volts | Source bulk voltage |
| $V_{D,SAT}$ | Volts | Drain voltage at which drift velocity saturates |
| E_{SAT} | Vm^{-1} | Field at which drift velocity saturates |
| λ | cm | Characteristic length of the electric field |
| α | cm^{-1} | Impact ionization coefficient |
| I_d | A | Drain current |
| I_{SUB} | A | Substrate current |
| w | Joule | Average electron energy |
| w_0 | Joule | Average electron energy at thermal equilibrium. |
| τ_w | Sec. | Energy relaxation time. |
| V_T | Volts | Threshold voltage. |
| ϕ_f | Volts | Fermi potential. |

| | | |
|--------------|-------------------|--|
| ϕ_{st} | Volts | Surface potential at strong inversion. |
| ψ_s | Volts | Surface potential . |
| w | meter | Depletion width. |
| W_s | meter | Source depletion width. |
| W_D | meter | Drain depletion width. |
| ϵ_y | Vm^{-1} | Normal electric field |
| ϵ_x | Vm^{-1} | Lateral electric field. |
| Q_i | Cm^{-2} | Inversion layer charge. |
| Q_B | Cm^{-2} | Bulk charge. |
| Q_s | Cm^{-2} | Surface charge. |
| Z | meter | Channel width. |
| μ_p | $m^2V^{-1}s^{-1}$ | Hole mobility. |
| μ_n | $m^2V^{-1}s^{-1}$ | Electron mobility. |
| ϵ_s | Fm^{-1} | Permittivity of silicon. |
| A_0 | cm^{-1} | Empirical constant. |
| B_0 | V/cm | Empirical constant. |
| v_d | ms^{-1} | Drift velocity. |
| d_j | m | Junction depth. |
| N_A | m^{-3} | Substrate doping |
| N_{SD} | m^{-3} | Source and drain Doping |

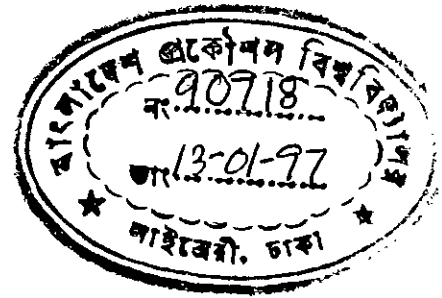
LIST OF FIGURES

| | | |
|-----|--|----|
| 1.1 | Structure of metal oxide semiconductor..... | 2 |
| 1.2 | Energy band diagram of a p-type substrate..... | 4 |
| 1.3 | Energy band diagram of a p-type substrate at higher voltage..... | 6 |
| 1.4 | Energy band diagram of a p-type substrate at the onset of strong inversion..... | 7 |
| 1.5 | Effect of hot-carrier in MOSFET..... | 14 |
| 2.1 | Simplified diagram of an n-channel MOSFET..... | 24 |
| 2.2 | Simplified diagram of after pinch-off reached | 27 |
| 2.3 | Current component due to bipolar transistor action in MOSFET..... | 42 |
| 3.1 | Drain current vs. drain voltage characteristics..... | 47 |
| 3.2 | Drain current vs. gate voltage characteristics..... | 48 |
| 3.3 | Electric field vs. distance normalized by characteristic length..... | 49 |
| 3.4 | Impact ionization coefficient vs. distance normalized by characteristic length..... | 50 |

| | | |
|------|--|----|
| 3.5 | Impact ionization co-efficient as a function of constant local field..... | 51 |
| 3.6 | Ionization coefficient vs. inverse of electric field..... | 54 |
| 3.7 | Parameter B vs. the inverse of characteristic length..... | 55 |
| 3.8 | Substrate current characteristics according to non-local impact ionization model taking $V_{DS} = 5$ Volts..... | 58 |
| 3.9 | Substrate current characteristics according to non-local impact ionization model taking $V_{DS} = 4$ Volts..... | 59 |
| 3.10 | Effect of substrate current on depletion width..... | 61 |
| 3.11 | Effect of substrate current on base emitter voltage..... | 62 |
| 4.1a | A flowchart illustrating the procedure of computing substrate current characteristics..... | 68 |
| 4.1b | A flowchart of a subprogram illustrating the procedure of finding surface potential..... | 69 |

CHAPTER 1

INTRODUCTION



1.1 MOS TRANSISTORS FUNDAMENTALS

The MOS transistor is a four-terminal device in which the lateral current flow is controlled by the externally applied vertical electric field. A typical MOS transistor has four-terminals: source, gate, drain and substrate. A n-channel enhancement MOSFET consists of a relatively lightly doped P type substrate into which two heavily doped n regions are diffused which act as source and drain respectively. When a positive voltage is applied to the gate with respect to the substrate, mobile negative charge is induced in the semiconductor below the semiconductor oxide interface. The negative carriers provide a conduction channel between the source and the drain.

The application of a voltage across the MOS capacitor establishes an electric field between the plates. The penetration of the field into the semiconductor produces a potential barrier beneath the surface where the depth of penetration depends on the doping density[1]. Thus

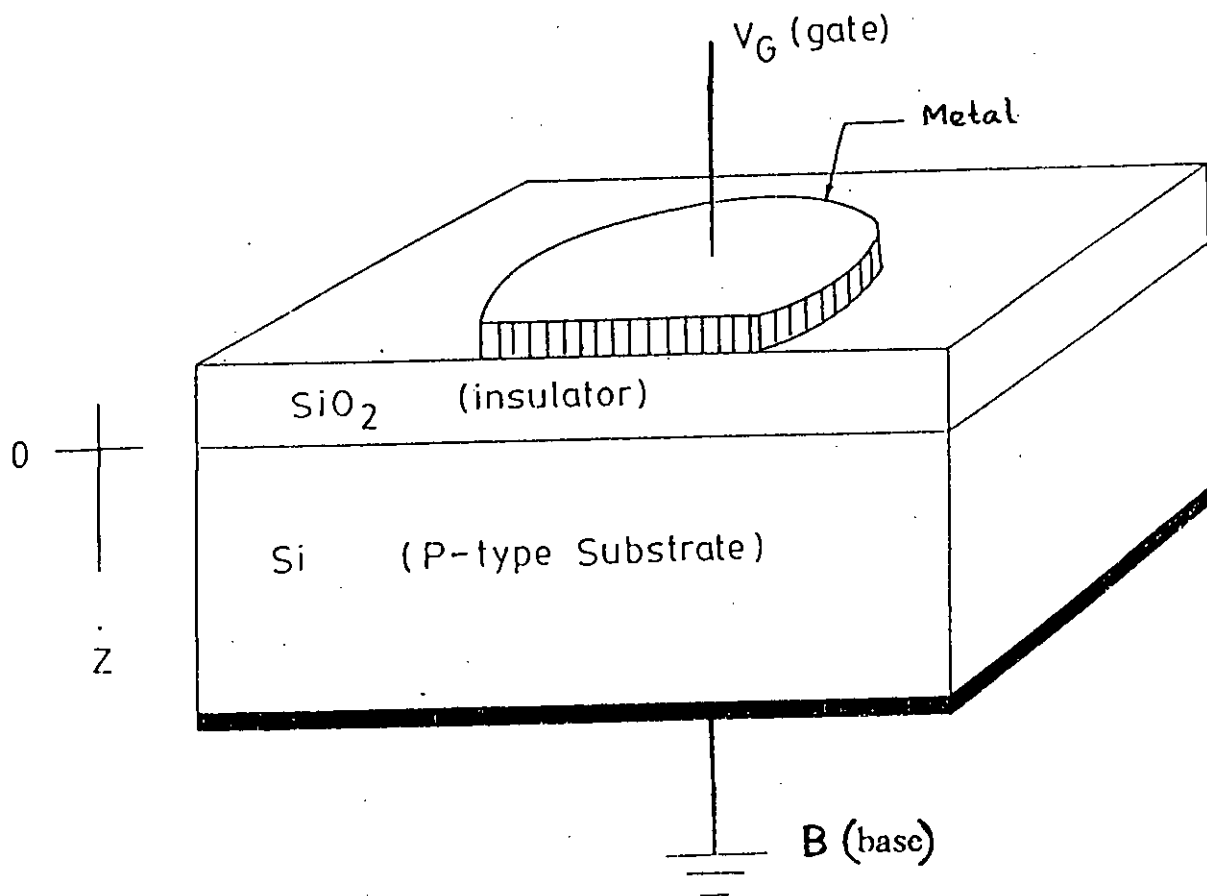


Fig.1.1. Structure of metal oxide semiconductor

$$V = \text{voltage across oxide, } V_o + \text{surface potential, } \Psi_s \quad (1.1)$$

The threshold voltage V_T of a MOSFET is defined as the minimum voltage required to induce the conduction channel. When a gate voltage equal to V_T is applied to a MOSFET it produces a large band bending which may cause the band gap energy E_i to cross over the constant-Fermi level by an amount ϕ_f at or near the Silicon Surface (Fig. 1.3). When this happens an inversion layer of width w_i is formed at the silicon surface.

For the condition of the onset of strong inversion, it is necessary to establish a higher inversion carrier density that corresponds to a surface potential of-

$$\Phi_{Si} = 2\Phi_f + 6\Phi_T \quad (1.2)$$

Where,

$$\phi_f = \frac{E_F - E_i}{q} = 2 \frac{kT}{q} \ln \frac{N_a}{n_i} \quad (1.3)$$

and

$$\phi_T = \frac{kT}{q} \quad (1.4)$$

Here, n_i is the intrinsic carrier concentration, E_F is the Fermi energy level and E_i is the intrinsic energy level.

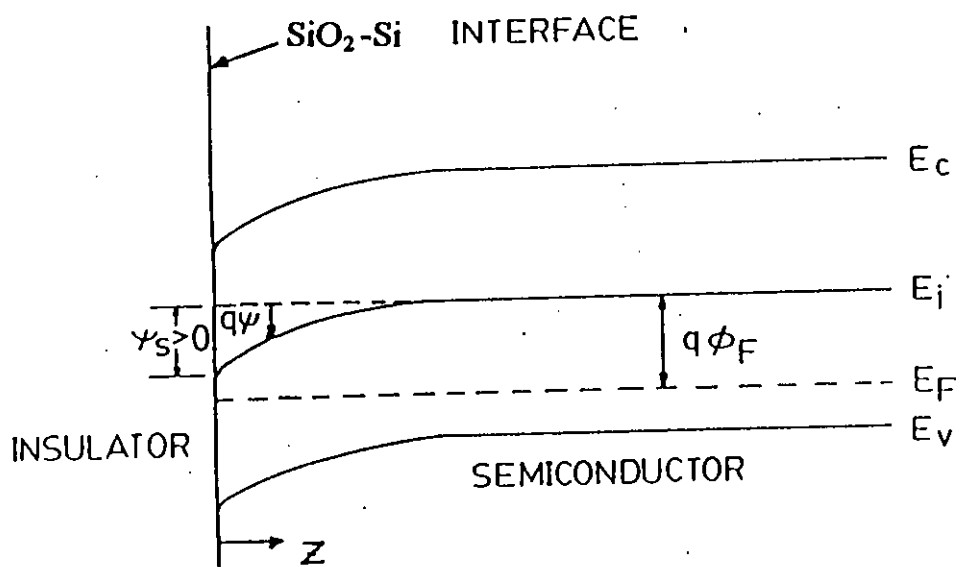


Fig.1.2. Energy band diagram of a p-type substrate

The corresponding width of the surface depletion region of the induced junction is-

$$x_{dm} = \sqrt{\frac{2k_s \epsilon_0 \phi_{si}}{qN_a}} \quad (1.5)$$

where,

k_s = Dielectric constant of semiconductor

ϵ_0 = Free space permittivity

N_a = Density of acceptor ions in substrate.

In figure 1.4, the left side of X_I remains n type whereas the right side remains P side. So, at the left side of X_I a region of inversion layer of width X_I and at the right side of X_I a surface depletion region of width X_d is produced which extends upto bulk. If we apply a large voltage so that $\psi_s > \phi_{si}$ then the increase of ψ_s is added to the difference of E_r and E_i and a small increase of ψ_s produces a large increase of electrons at the surface, according to the relation of

$$n = n_i e^{\frac{q\psi}{kT}} \quad (1.6)$$

$$p = p_i e^{-\frac{q\psi}{kT}} \quad (1.7)$$

Therefore, the surface inversion layer is acting like a narrow n^+ layer, and the induced junction resembles on n^+p junction for a large positive gate voltage.

However, all induced charge will be in the inversion layer after strong inversion,

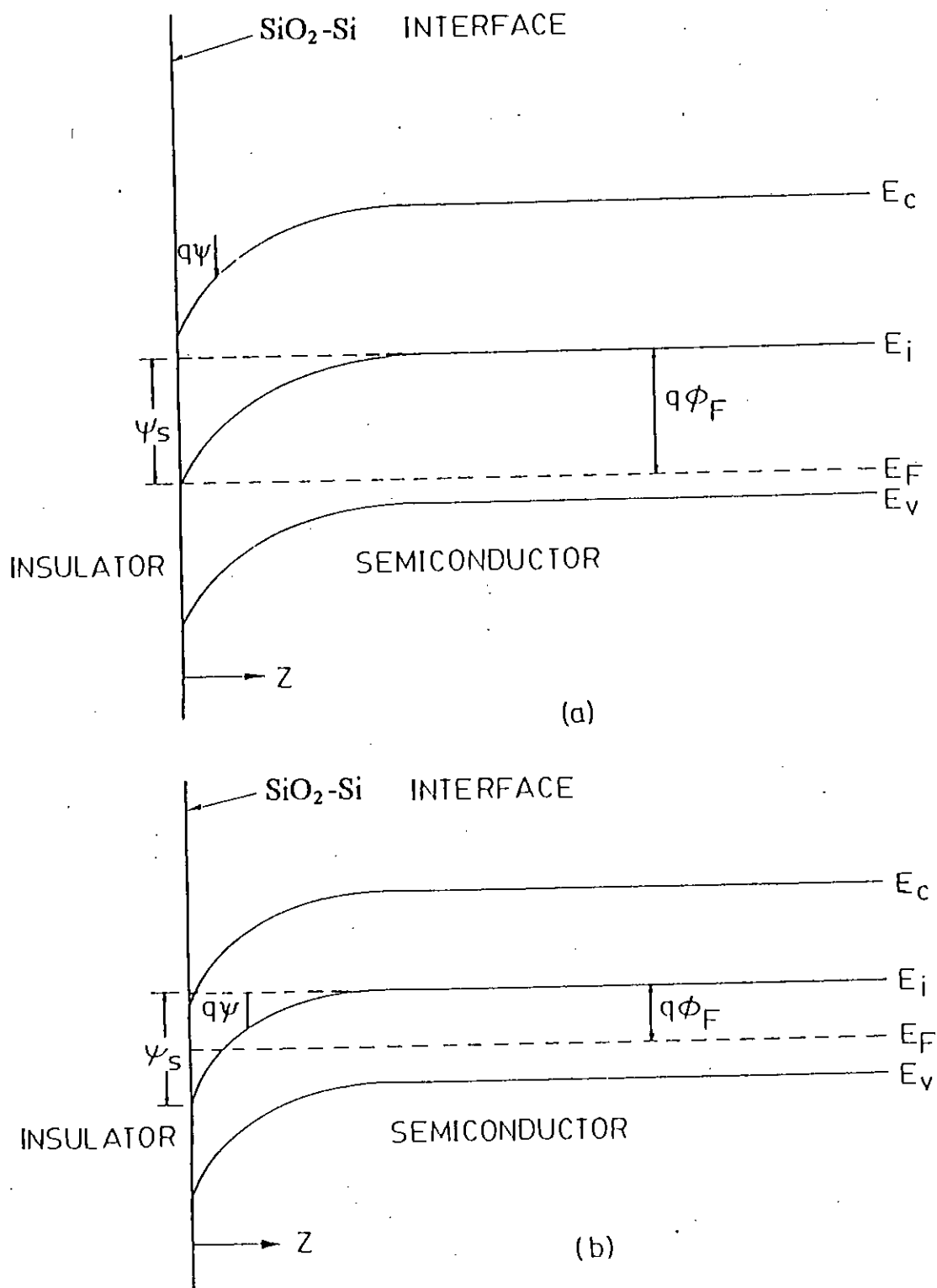


Fig. 1.3 Energy band diagram of p-type substrate at higher gate voltage
 (a) Depletion (b) Inversion

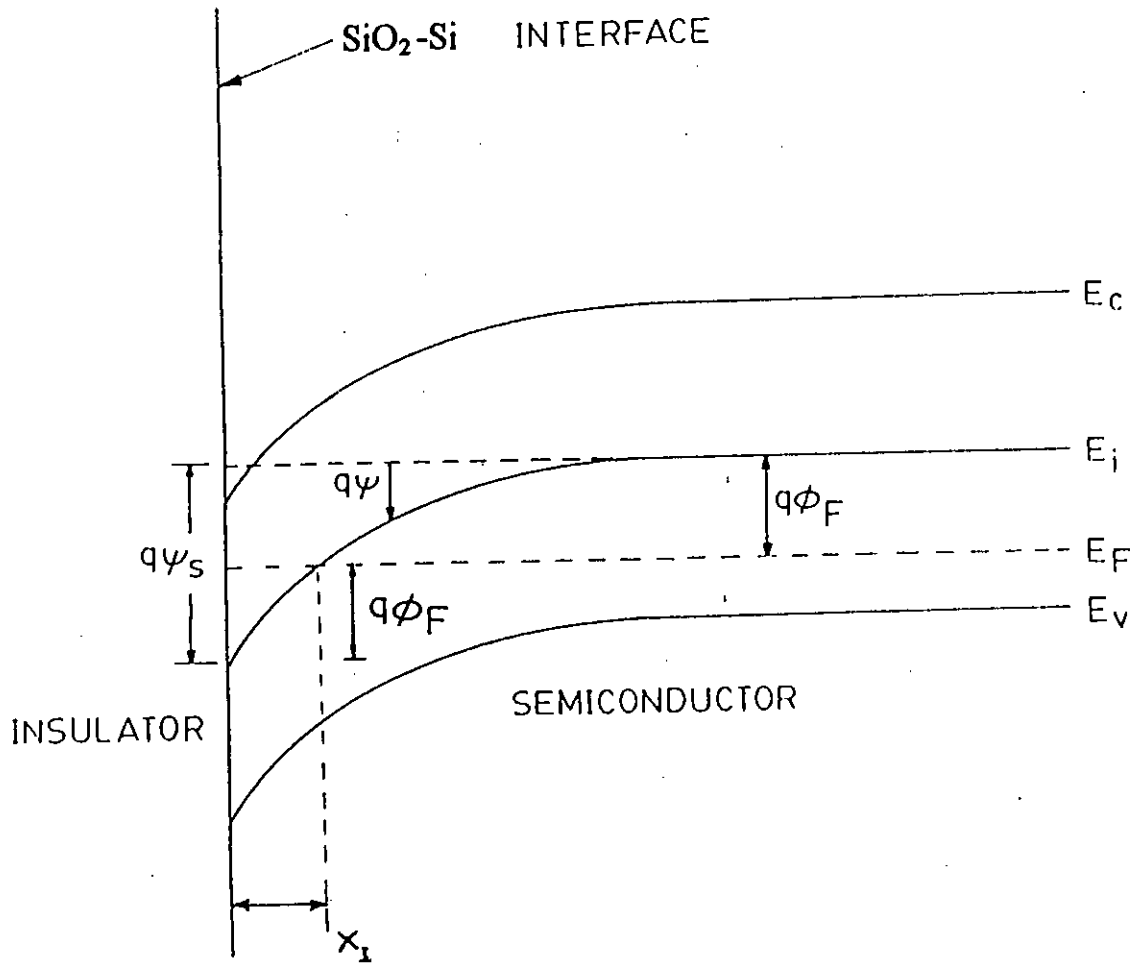


Fig.1.4. Energy band diagram of a p-type substrate at the onset of strong inversion

and the charge inside the depletion layer will remain constant. With a depletion layer width of X_{dm} , the bulk charge Q_B becomes

$$Q_B = -qN_a X_{dm} \quad (1.8)$$

The charge balance equation in the surface region of a MOSFET can be written as

$$\begin{aligned} Q_s &= Q_I + Q_B \\ &= Q_G \end{aligned} \quad (1.9)$$

where, Q_s , Q_I , Q_G are total charge, inversion layer charge and gate charge respectively.

The applied gate voltage V_{GB} in a MOSFET is shared by the flat band voltage V_{FB} surface potential ψ_s and voltage across the oxide V_o and is given by

$$\begin{aligned} V_{GB} &= V_{FB} + \psi_s - \frac{Q_s}{C_o} \\ V_{GB} &= V_{FB} + \psi_s + \gamma \sqrt{\psi_s} \end{aligned} \quad (1.10)$$

where,

$$\gamma = \frac{\sqrt{2q \epsilon_s N_a}}{C_o} \quad (1.11)$$

and,

$$C_o = \frac{\epsilon_{ox}}{t_{ox}} \quad (1.12)$$

where, C_o , t_{ox} are oxide capacitance per unit area and oxide thickness respectively.

At the onset of strong inversion $Q_I \ll Q_B$, then equation (1.10) reduces to $Q_s = Q_I + Q_B$. So the threshold voltage can be represented as

$$V_T = V_{FB} + \psi_s - \frac{Q_B}{C_o} \quad (1.13)$$

Now the inversion layer charge at a gate voltage above threshold is given by

$$Q_I = -C_o (V_{GB} - V_T) \quad (1.14)$$

After formation of channel, if a drain voltage V_{DS} greater than saturation voltage V'_{DS} is applied between drain and source, the electron density near the drain will be reduced at $V_{DS} > V'_{DS}$, pinch off will occur near the drain. After the pinch off at the channel the effective channel length of a MOSFET differs from its physical channel length.

Depending on the physical length of the channel, MOSFET are categorized into long and short channel MOSFET. When the channel length L is much longer than the sum of source and drain depletion width ($w_s + w_D$) (Fig.3.1) then it is called long channel MOSFET and when $L < (w_s + w_D)$ then the MOSFET is called short

channel MOSFET. The depletion width w_s and w_D are controlled by bias voltage V_{DB} and V_{SB} respectively where V_{DB} represents drain bulk bias and V_{SB} the source bulk bias. In short channel MOSFET's the difference between effective and physical channel length increases with the increase of drain source voltage, whereas in long channel it is almost constant.

1.2 EFFECT OF SUBSTRATE BIAS:

Generally the source and the substrate terminals of a MOSFET are directly grounded. But if a negative voltage is applied to the P type substrate with respect to the source (n^+), a reverse bias voltage, V_{SB} will be across the induced junction between the channel and body and also between the source and the substrate junction. In this case the inversion layer substrate junction will act as a field induced p junction and the source substrate junction will act as a regular pn junction. In either case the depletion region is widened and the threshold voltage required to achieve inversion must be increased to accommodate the large Q_B . In this case, the bias will shift the quasi fermi level at the source by V_{SB} . So the surface potential at the source during strong inversion can be modified as

$$\psi_s = V_{SB} + \phi_{SI} \quad (1.15)$$

as the bulk charge becomes

$$Q_B = -[2q\epsilon_s N_a (V_{SB} + \phi_{Si})]^{1/2} \quad (1.16)$$

Therefore, the increased differential charge is

$$\Delta Q_B = -(2q\epsilon_s N_a)^{1/2} [(V_{SB} + \phi_{Si}) - \phi_{Si}^{1/2}] \quad (1.17)$$

To reach the strong inversion, the applied gate voltage must be increased to compensate for ΔQ_B . Therefore,

$$\Delta V_T = -\frac{\Delta Q_B}{C_o}$$

$$\Delta V_T = \frac{(2q\epsilon_s N_a)^{1/2}}{C_o} [(V_{SB} + \phi_{Si})^{1/2} - \phi_{Si}^{1/2}] \quad (1.18)$$

When a positive V_{BS} is applied to the substrate with respect to source then the situation will be reversed. The source substrate and channel substrate junction both will be forward biased and to maintain the charge balance equation the inversion layer charge must be increased, whereas the depletion layer charge is decreased. So in an n channel MOSFET, V_{BS} must be zero or negative to avoid the forward bias of the source junction.

1.3 ADDITIONAL FEATURES OF SHORT CHANNEL

MOSFET:

When the dimensions of a MOSFET are reduced the distinct features are seen in device characteristics. First the drain current is found to increase with the drain voltage due to channel length modulation beyond pinch off. This is in contrast with I-V curve of a long channel MOSFET, where the drain current becomes constant after the pinch off condition. But the output current in short channel MOSFET does not saturate. The second feature of a short channel MOSFET can be seen in the subthreshold region where the gate loses control over the drain current. In other words, the output drain current can't be reduced to zero i.e. can't be turned off. The third feature is that due to the presence of velocity saturation the drain current in short channel MOSFET for a fixed drain-source voltage is smaller than the corresponding drain current in long channel MOSFET. The fourth distinct feature of a short channel MOSFET is the shift of its threshold voltage with the channel length as well as drain bias voltage. Whereas, the threshold voltage of a long channel MOSFET is not a function of either drain bias or channel length.

1.4 AVALANCHE BREAKDOWN AND HOT CARRIER

EFFECT:

In the reverse bias drain, to substrate junction, the electric field may be quite high and electron hole pairs will be generated due to impact ionization. The mechanism of avalanche breakdown of a junction involves the impact ionization of host atoms by energetic carriers. Normal lattice scattering event can result in the creation of electron hole pair if the carrier being scattered has sufficient energy. If a large reverse voltage is applied across a p n junction, the electric field in the transition region becomes large and an electron entering from the p side may be accelerated to high kinetic energy to cause an ionizing collision with the lattice. A single such interaction results in carrier multiplication. The degree of multiplication can become very high if carriers generated within the transition region also has ionizing collisions with the lattice. This is an avalanche process, since each incoming carrier can initiate the creation of a large number of new carriers.

Most of the electrons generated by the avalanche multiplication are normally attracted by the drain and the holes generated by multiplication can flow to the substrate, giving rise to a large substrate current. The electrons generated in the drain depletion layer are also attracted to the positive gate voltage, as shown in

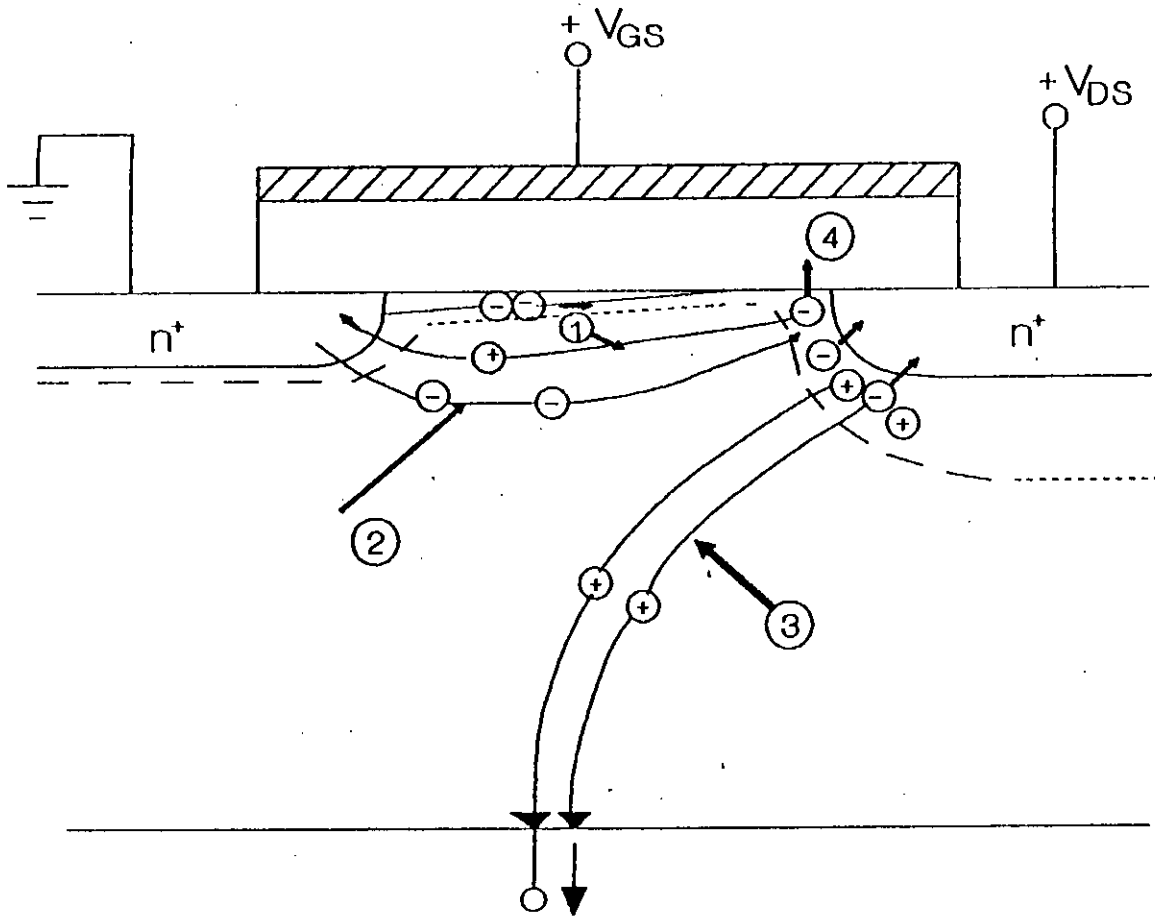


Fig.1.5. Effects of hot carriers in MOSFET
 1.Holes that flow to the source
 2.Electrons that flow to the drain
 3.Holes that flow to the substrate
 4.Electrons that tunnel into the oxide

figure 1.5. If these electrons have an energy greater than 1.5 eV, they may be able to tunnel into the oxide or to surmount the silicon oxide potential barrier to produce a gate current. In either case, electrons can be trapped inside the gate oxide, thus changing the threshold voltage and the current voltage characteristics. This is not desirable and should be avoided. The hot carrier effects can be minimized if the electric field of the function can be reduced. This can be accomplished by using the lightly doped drain structure. The lightly doped drain design improves the performance. It has a higher breakdown voltage, and the substrate current is reduced by a factor of 30.

1.5 REVIEW OF RECENT WORKS ON SUBSTRATE CURRENT MODELING OF MOSFET

Hot-carriers generated by the very large electric fields of the drain region create serious reliability problems. One manifestation of the presence of such hot-carriers is the substrate current resulting from impact ionization. A number of models on the substrate current of MOSFET's have been developed in the last few years. D.P. Kennedy and A Philips [2] in 1973 first developed a source-drain breakdown model and suggested that the positive feedback effect involving bipolar transistor action is the main breakdown mechanism in short channel MOSFET. In 1977 T. Toyable [3] developed a two dimensional avalanche breakdown model of short channel MOSFET. Later Fu-chien Hsu, Simon Tam [4] derived a simple analytical breakdown model that combines the effects due to ohmic drop caused by the substrate current and the positive feedback effect of the substrate lateral bipolar transistor. They pointed out that drain source breakdown in most short channel MOSFET's is neither simple junction avalanche breakdown nor source to drain punch through but it is avalanche-induced breakdown and two conditions must be satisfied before the breakdown can occur. One is the emission of minority carrier into the substrate from the source and other is the sufficient avalanche multiplication to cause significant positive feedback.

The most widely implemented substrate current models in device simulators, such as PISCES[5], rely on the local electric field to determine the amount of impact ionized carrier generation within devices. These models adopt a simplification equivalent to assuming that the carrier instantaneously acquires the steady-state energy associated with the field at each grid point. This assumption is clearly violated in regions of rapidly varying electric fields. As a result, when attempting to use these local-field models, it is a common practice among users to modify the coefficient of the impact ionization rate in order to obtain agreement between the simulated and experimentally measured substrate currents. In 1982, R.K. Cook and J. Frey [6] presented a technique for studying energy transport effects in submicron-scale semiconductor devices using a two-dimensional numerical simulation. Using this model, it was found that the inclusion of energy transport effects is very important for the accurate simulation of submicron-scale GaAs MESFET's, but is not as important for Si devices. In 1988, N. Goldsman and J. Frey [7] presented a strategy for accurate and efficient application of the energy transport method to determine average electron energy, the most critical quantity affecting many types of device degradation. In 1989, C.G. Hwang, R.W. Dutton [8] investigated the non-equilibrium effects of hot carrier to analyze avalanche generation. In 1992, V.M. Agostinelli, T.J. Bordelon [5] reported a two-

dimensional substrate current model and it has shown to more accurately estimate the substrate currents in devices fabricated by different technology. In this work, we propose a nonlocal impact ionization model applicable for the drain region where electric field increases exponentially and using this model, an expression for substrate current model is developed to explain experimental data in a satisfactory manner.

1.6 OBJECTIVE OF THIS THESIS:

The main objective of this research is to develop an improved model for the substrate current to explain the experimental data. The substrate current model is developed through the development of nonlocal impact ionization model. This impact ionization model is obtained from the analytical solution of the energy conservation equations for electrons.

1.7 SUMMARY OF THE DISSERTATION

Chapter one deals with the fundamental concepts of MOSFET including its threshold voltage, substrate bias (body) effect and various undesirable effects. The effect of hot carrier and substrate current produced by the mechanism of avalanche multiplication that drives a MOSFET into the breakdown mode have also been described briefly in the chapter. A through literature review related to this work has been carried out. The objective of this work is also mentioned in this chapter.

In chapter two, an analytical expression for nonlocal impact ionization rate is developed from the analytical solution of the energy conservation equation for electrons. Analytical expressions for finding the drain current are also presented in this chapter. A new substrate current model is developed using these expressions. The effects of this substrate current on the channel current is also explained in this chapter.

In chapter three of the thesis ,results of the developed non local impact ionization model and the substrate current model are presented and a computer program scheme to study the characteristics are also presented. A brief discussion on the results is also presented in this chapter.

The final chapter contains the concluding remarks with suggestions for further improvement.

CHAPTER 2

HOT-CARRIER INDUCED SUBSTRATE CURRENT MODEL

2.1 INTRODUCTION:

For the reverse-bias drain-to-substrate junction, the electric field at drain end may be quite high and electron hole pairs will be generated due to impact ionization. Normal lattice-scattering event can result in the creation of electron-hole pair if the carrier being scattered has sufficient energy. In this case, an electron entering from the p side may be accelerated to high kinetic energy to cause an ionizing collision with the lattice. A single such interaction results the carrier multiplication. Hot-carrier induced degradation has been one of the main concerns in scaled down MOSFET's. One manifestation of the presence of such hot-carriers is the substrate current resulting from impact ionization of carriers in the high field region of the drain. The measurement of substrate current has become an important and widely used method for monitoring the presence of energetic carriers. For this reason, the substrate current itself has been used as a parameter in modeling device reliability.

The impact ionization events generally occur near the drain where highly nonuniform electric field exists. The channel electrons experiencing rapid change of electric field do not reach their stationary state transport. The non-stationary transport of electrons could affect the impact ionization. However, quantitative argument of the non-local impact ionization in MOSFET's is still lacking. In this work, a nonlocal impact ionization model is developed from the analytical solution of the energy conservation equation for electrons in section (2.3)

From the non-local impact ionization model, a new analytical model for substrate current of n-channel MOSFET's is derived in section (2.4). Then the model is compared with the experimentally measured substrate current. The possible effects of the substrate current on MOS transistor is explained in section (2.5).

2.2.1 CURRENT-VOLTAGE RELATION IN MOS TRANSISTORS

A schematic diagram of an n-channel MOSFET is shown in Fig. 2.1 in which bias voltages are included. To simplify our analysis, we have grounded the source and substrate terminals. Let us consider a small section at y of the transistor in Fig. 2.1 under the condition that the gate voltage is greater than threshold voltage so that significant amounts of mobile carriers are induced in the inversion layer.

Then the total current in y -direction can be written as

$$\begin{aligned} I_D &= I_D(\text{drift}) + I_D(\text{diffusion}) \\ &= I_{D1} + I_{D2} \end{aligned} \quad (2.1)$$

Where, I_{D1} and I_{D2} can be expressed as [1],

$$I_{D1} = \frac{\mu_n W C_o}{L} \left[(V_{GB} - V_{FB})(\psi_{SL} - \psi_{SO}) - \frac{1}{2}(\psi_{SL}^2 - \psi_{SO}^2) - \frac{2}{3}\gamma(\psi_{SL}^{\frac{3}{2}} - \psi_{SO}^{\frac{3}{2}}) \right] \quad (2.2)$$

and

$$I_{D2} = \frac{\mu_n W \phi_T C_o}{L} \left[(\psi_{SL} - \psi_{SO}) + \gamma(\psi_{SL}^{1/2} - \psi_{SO}^{1/2}) \right] \quad (2.3)$$

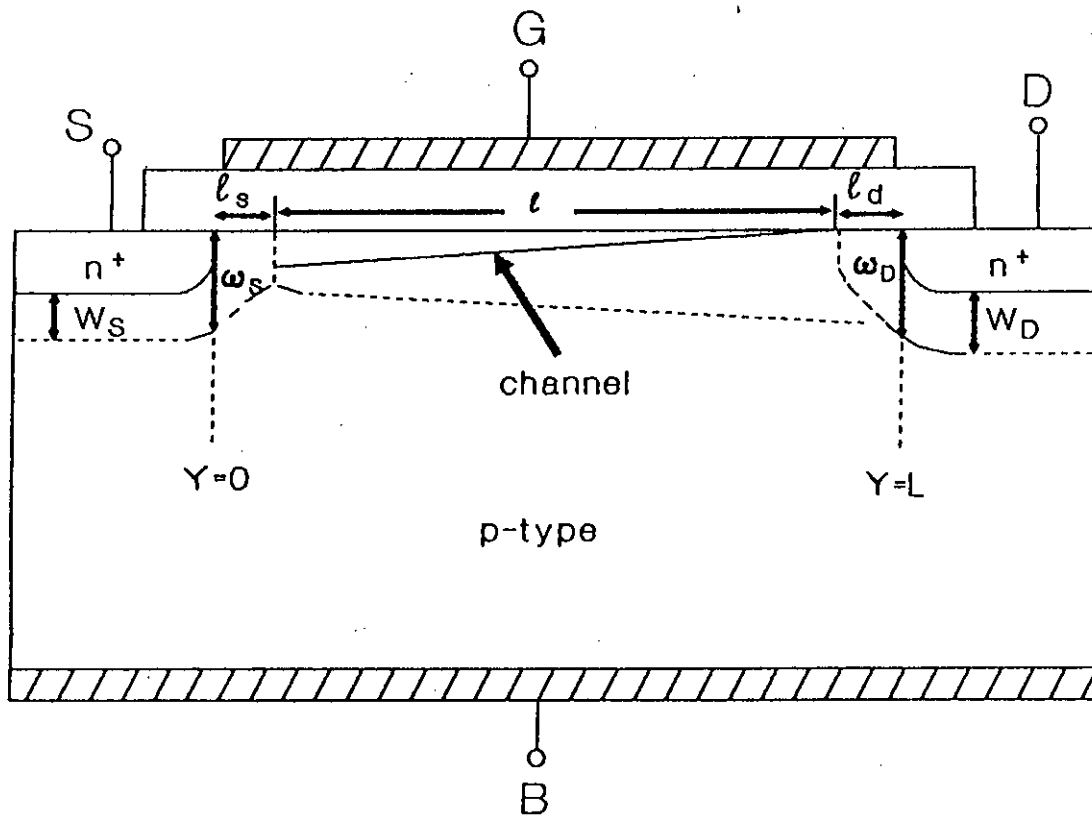


Fig. 2.1 Simplified diagram of a n-channel MOSFET

Equation (2.2) and (2.3) are the drift and diffusion components. What remains to be

found are the boundary conditions of the surface potentials at the source and the drain.

The surface potentials at the source and drain are found from the iterative value of the

following equations[1]

$$\psi_{so} = V_{GB} - V_{FB} - \gamma \left[\psi_{so} + \phi_T \exp\left(\frac{\psi_{so} - 2\phi_f - V_{SB}}{\phi_T}\right) \right]^{1/2} \quad (2.4)$$

and,

$$\psi_{SL} = V_{GB} - V_{FB} - \gamma \left[\psi_{SL} + \phi_T \exp\left(\frac{\psi_{SL} - 2\phi_f - V_{DB}}{\phi_T}\right) \right]^{1/2} \quad (2.5)$$

Using the computed values of surface potential, the total drain current can now be computed.

2.2.2 DETERMINATION OF DRAIN SATURATION VOLTAGE

In the region of strong inversion, the diffusion term is not important so that we may use equation (2.2) to represent the current of the transistor. The surface potential is the sum of ϕ_{si} and the appropriate bias. Thus,

$$\psi_{so} = \phi_{si} + V_{SB} \quad (2.6)$$

$$\psi_{SL} = \phi_{si} + V_{DB} \quad (2.7)$$

With these conditions, equation (2.2) becomes,

$$I_D = \frac{W}{L} \mu_n C_0 \left\{ (V_{GB} - V_{FB} - \phi_{si}) V_{DS} - \frac{1}{2} V_{DS}^2 - \frac{2}{3} \left[(\phi_{si} + V_{SB} + V_{DS})^{3/2} - (\phi_{si} + V_{SB})^{3/2} \right] \right\} \quad (2.8)$$

At the pinch-off point,

$$\left. \frac{dI_D}{dV_{DS}} \right|_{V_{D,SAT}} = 0$$

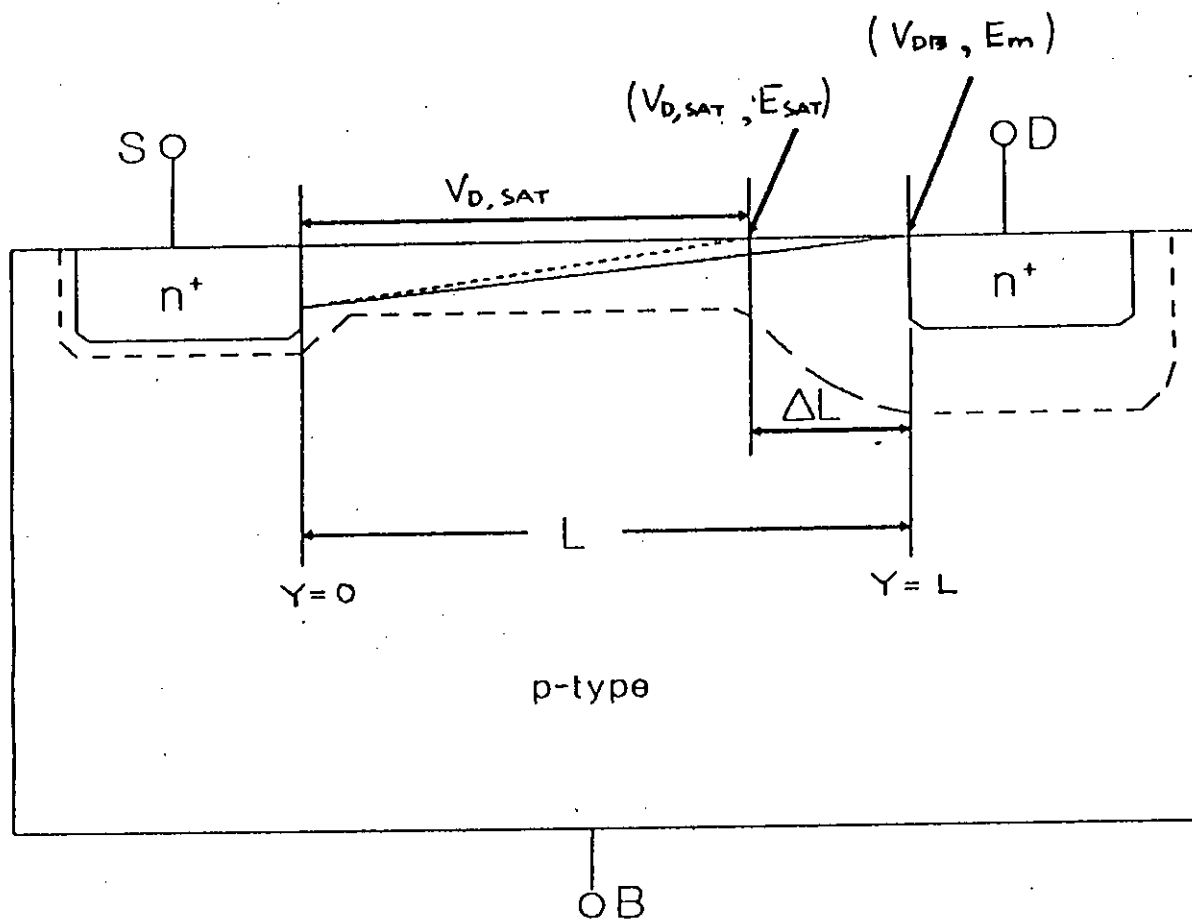


Fig. 2.2 Simplified diagram of after pinch-off reached

$$\left(V_{GS} - V_{FB} - \phi_{si} \right) - V_{D,SAT} - \gamma \left(\phi_{si} + V_{SB} + V_{d,SAT} \right)^{1/2} = 0 \quad (2.9)$$

Let,

$$a = V_{GS} - V_{FB} - \phi_{si} \quad (2.10)$$

$$b = \phi_{si} + V_{SB} \quad (2.11)$$

Then equation (2.9) reduces to

$$a - V_{D,SAT} - \gamma \left(b + V_{D,SAT} \right)^{1/2} = 0$$

or,

$$V_{D,SAT}^2 - V_{D,SAT} \left(\gamma^2 + 2a \right) + \left(a^2 - b\gamma^2 \right) = 0$$

or,

$$V_{D,SAT} = a + \frac{\gamma^2}{2} - \gamma \sqrt{a + b + \frac{\gamma^2}{4}} \quad (2.12)$$

Substituting equation (2.10) and (2.11), we get

$$V_{D,SAT} = V_{GS} - V_{FB} - \phi_{si} + \frac{\gamma}{2} - \gamma \sqrt{V_{GS} - V_{FB} + V_{SB} + \frac{\gamma}{4}} \quad (2.13)$$

This is the drain voltage at which drain current saturates for a particular values of V_{GS} .

2.3.1 LOCAL-FIELD MODEL OF IMPACT IONIZATION

In the case of high electric field along the channel, carriers that are injected into the depletion layer are accelerated by the high field, and some of them may gain enough energy to cause impact ionization. An impact ionization co-efficient, α is defined as the number of impact ionization events caused by an electron per unit length along the electric field. In uniform electric field, the co-efficient is expressed as [9]

$$\alpha(E) = A_0 \exp(-B_0 / E) \quad (2.16)$$

In the exponential expression, E is the electric field component parallel to the current density which can say as field parallel to the Si/SiO₂ interface. The field component perpendicular to the current flow does not cause ionization since the carriers only gain energy from the field component parallel to their motion. Further details is shown in appendix-B.

Various authors have determined A_0 and B_0 experimentally [10]. Many authors used different values of A_0 and B_0 [11-14]. It is widely accepted that these

parameters are in the range of $6.2-7.03 \times 10^5 \text{ cm}^{-1}$ for A_0 and $1.08-1.231 \times 10^6 \text{ V/cm}$ for B_0 .

Equation (2.16) is developed under the concept of an uniform field. The rapid spatial variation of electric field prevents carriers from reaching a steady-state equilibrium with the local electric field. So the assumption of steady-state energy associated with the field is not proper. Thus it has been employed in device simulators by treating A_0 , B_0 as fitting parameters to express impact ionization in scaled devices, in where strong nonuniformity of electric field exists.

According to the pseudo two-dimensional model [15], the electric field in the velocity saturation region of MOSFET's is expressed by

$$E = E_{\text{sat}} \exp(x / \lambda) \quad (2.17)$$

Where,

E = Electric field parallel to the Si/SiO₂ interface

x = Distance from a velocity saturation point

E_{sat} = Field at which drift velocity saturates.

λ = Characteristic length for the electric field.

It depends on geometrical sizes of MOSFET.

Using equations (2.16) and (2.17) , the impact ionization model (\propto Vs. x/λ) can be developed by determining the variation of electric field with x/λ .

2.3.2 NONLOCAL IMPACT IONIZATION MODEL

To ascertain average electron energy w , a simple energy transport equation is derived. Using common definition of moments in the electron distribution function we obtain [7]

$$\frac{\delta w}{\delta t} + v \cdot \nabla w = e(v \cdot E) - \frac{\nabla}{n} \cdot (nkT_e \cdot v) - \frac{\nabla}{n} \cdot Q + \left(\frac{dw}{dt}\right)_{\text{collision}} \quad (2.18)$$

Where,

E = Electric field

w = Average electron energy

T_e = Electron temperature

v = Electron drift velocity

n = Electron concentration

Q = Diffusive heat flow term

The left hand side of equation (2.18) is the rate at which energy changes within a differential volume element of electron gas as it moves along the direction of electron flow. The right-hand side describes how individual forces contribute to change the total energy of the volume element. The rate at which work is done on the volume element by the electric field is described by the first term to the right of the equal sign. The $nkT_e.v$ term describes the work done by the electron gas as it exerts pressure and is deformed ; the Q term describes the rate at which energy is removed from the element by the conduction of heat.

Equation (2.18) contains five unknown : w , T_e , v , Q , and n . The $\delta w/\delta t$ term is neglected by assuming that the carrier acquires the steady-state energy associated with the field at each grid point. If we make the approximation that the electron distribution function is symmetrical in momentum space, then $(\nabla/n).Q = 0$ and if there is no generation or recombination $\nabla.nv=0$. Furthermore , $w \approx 3/2kT_e$. So that $kT_e \approx 2/3w$ and three unknowns are removed . Then we can write the energy transport equation in one dimension as

$$\frac{\delta w}{\delta x} = eE(x) - \frac{2}{3} \frac{\delta w}{\delta x} + \frac{1}{v} \left(\frac{dw}{dt} \right)_{\text{coll}} \quad (2.19)$$

The collision term can be evaluated as

$$\left(\frac{dw}{dt}\right)_{\text{coll}} = \frac{w - w_0}{\tau_w} \quad (2.20)$$

Where w_0 and τ_w are average electron energy at thermal equilibrium and energy relaxation time for electrons respectively. From equations (2.19) and (2.20), we get

$$\frac{5}{3} \frac{\delta w}{\delta x} = eE(x) - \frac{w - w_0}{v\tau_w} \quad (2.21)$$

The electron current density expressed as $j = env_n$ is constant provided the electron-hole generation rate is negligible compared to the channel current. This means that both j and n are also constant in the velocity saturation region where the drift velocity, v_n has the constant value v_{sat} . Then the equation (2.21) can be written as

$$\frac{5}{3} \frac{\delta w}{\delta x} = eE(x) - \frac{w - w_0}{v_{\text{sat}}\tau_w}$$

or,

$$\frac{\delta w}{\delta x} = \frac{3}{5} eE - \frac{w - w_0}{\frac{5}{3} v_{\text{sat}}\tau_w} \quad (2.22)$$

Then,
$$\frac{\delta w}{\delta x} = \frac{3}{5} eE - \frac{w - w_0}{l_w}$$

where,

$$l_w = \frac{5}{3} v_{sat} \tau_w$$

or,
$$\frac{\delta w}{\delta x} + \frac{1}{l_w} w = \frac{3}{5} eE + \frac{w_0}{l_w} \quad (2.23)$$

with operator notation, we write the equation as

$$\left(D + \frac{1}{l_w} \right) w = \frac{3}{5} eE + \frac{w_0}{l_w}$$

The appropriate integrating factor is

$$u = e^{\int \frac{1}{l_w} dx} = e^{\frac{x}{l_w}}$$

and the general solution consists of two parts

(I) Complementary solutions; w_c :

$$w_c = \frac{C}{u} = ce^{-x/l_w}$$

(ii) Particular integral, w_p :

$$w_p = \frac{1}{u} \int u \left(\frac{3}{5} eE + \frac{w_0}{l_w} \right) dx$$

or,
$$w_p = e^{-\frac{x}{l_w}} \int e^{\frac{x}{l_w}} \left[\frac{3}{5} eE_{sat} e^{\frac{x}{\lambda}} + \frac{w_0}{l_w} \right] dx$$

$$\text{or, } w_p = w_0 + \frac{\frac{3}{5} e l_w E_{sat} e^{\frac{x}{\lambda}}}{1 + \frac{w}{\lambda}}$$

$$\text{or, } w_p = w_0 + \frac{\frac{3}{5} e l_w E(x)}{1 + l_w / \lambda}$$

The general solution of equation (2.23) is then

$$w = w_c + w_p$$

$$\text{or, } w(x) = c e^{-\frac{x}{l_w}} + w_0 + \frac{\frac{3}{5} e l_w E(x)}{1 + l_w / \lambda} \quad (2.24)$$

At $x=0$, equation (2.24) becomes to

$$w(0) = c + w_0 + \frac{\frac{3}{5} e l_w E_{sat}}{1 + l_w / \lambda}$$

$$\text{or, } c = w(0) - w_0 - \frac{\frac{3}{5} e l_w E_{sat}}{1 + l_w / \lambda} \quad (2.25)$$

Substituting the integrating constant c into equation (2.24), we get

$$w(x) = w(0) e^{-\frac{x}{l_w}} + w_0 \left(1 - e^{-\frac{x}{\lambda}} \right) - \frac{3 e l_w E_{sat}}{5 (1 + l_w / \lambda)} e^{-\frac{x}{\lambda}} + \frac{3 e l_w E(x)}{5 (1 + l_w / \lambda)} \quad (2.26)$$

Where x is a distance from the velocity saturation point and e is electric charge.

Impact ionization occurs significantly in the region where the electric field exceeds 200 kv/cm. The average energy $w(x)$ in the region is larger than $w(0)$ and w_0 .

These facts allow us to simplify equation (2.26) as

$$w(x) \approx \frac{3}{5} \frac{e l_w E(x)}{1 + l_w / \lambda} \quad (2.27)$$

In uniform electric field, $\lambda \rightarrow \alpha$. Then w converge to $(3/5)e l_w E$; it is the average energy in uniform electric field, E .

Since impact ionization events are caused by high energy electrons, the impact ionization co-efficient in nonuniform field should be expressed as a function of the average electron energy rather than the local electric field model. Substituting $E = 5w / (3e l_w)$ into equation (2.16), ionization co-efficient can be expressed as a function of the average energy as

$$\alpha = A_0 \exp(-3 l_w e B_0 / 5w) \quad (2.28)$$

In exponentially increasing field, with the use of the energy given by equation (2.27), the impact ionization co-efficient becomes

$$\alpha(E) = A_0 \exp\left(-\frac{B(\lambda)}{E}\right) \quad (2.29)$$

where,

$$B(\lambda) = \left(1 + \frac{I_w}{\lambda}\right) B_0 \quad (2.30)$$

equation (2.29) indicates a linear relationship of $\log \alpha$ vs. $1/E$ characteristic length, λ as given by equation (2.30).

2.4 ANALYTICAL SUBSTRATE CURRENT MODEL

When the drain voltage becomes sufficiently high, an avalanche breakdown occurs within the pinch-off region. The generated holes are collected by the substrate terminal and constitute substrate current. The resulting current by this impact ionization process can be written as

$$I_{SUB} = \int_0^{\Delta L} I_D \alpha dx \quad (2.31)$$

Where ΔL is the length of the pinch-off region.

Using equation (2.16) and (2.17), equation (2.31) can be written as

$$\begin{aligned} I_{SUB} &= \int_0^{\Delta L} I_D A \exp(-B/E) dx \\ &= \int_0^{\Delta L} I_D A \exp\left[-b / \left(E_{SAT} \exp(x/\lambda)\right)\right] dx \end{aligned} \quad (2.32)$$

The voltage variation from pinch-off point to drain end can be expressed as

$$V(x) = V_{D,SAT} + \int_0^x E(x) dx$$

or,
$$V = V_{D,SAT} + \lambda E_{sat} \left(e^{x/\lambda} - 1 \right) \quad (2.33)$$

Substituting equation (2.33) into equation (2.32) and using the boundary condition

that

$$\text{At } x=0, \quad V=V_{D,sat}$$

$$\text{At } x=\Delta L, \quad V=V_{DB}$$

equation (2.31) can be reduced to

$$I_{SUB} = \frac{A}{B} I_D \left(V_D - V_{D,SAT} \right) \exp \left(\frac{-\lambda B}{V_D - V_{D,SAT}} \right) \quad (2.34)$$

Where, $V_{D,SAT}$ is the drain voltage at which drift velocity saturates.

2.5 EFFECTS OF SUBSTRATE CURRENT

The breakdown in MOSFET is not a simple junction avalanche breakdown rather it is a breakdown induced by avalanche multiplication. Two consecutive phases of breakdown occur in such a MOSFET. First, the reduction of threshold voltage is caused by the enhanced body effect (EBE) and then the sharp rise in drain current is initiated by the bipolar transistor action of the MOSFET.

2.5.1 Enhanced body effect

The physical mechanism of the enhanced body effect is that the holes, multiplied in the drain junction, bias the substrate spreading resistance when flowing towards the substrate terminal. The bias corresponds to a reduction in the channel region depletion width from w_0 which corresponds ($I_{SUB} = 0$) to w and thus releases a certain amount of bulk charge Q_B of ionized impurities, which was initially tied by the gate field. The reduction of the bulk charge implies a threshold lowering of the MOSFET. Hence the drain current will increase due to this effect.

The variation of depletion width, w with the substrate current is [16]:

$$w = \sqrt{\left(\frac{\epsilon_s r I_{sub}}{q l N_s}\right)^2 + w_0^2 \left(1 - \frac{R_{sub} I_{sub}}{\psi_c}\right) - \frac{\epsilon_s r I_{sub}}{q l N_s}} \quad (2.35)$$

Where,

$$w_0 = w(I_{sub} = 0) = \sqrt{\frac{2\epsilon_s \psi_c}{qN_s}} \quad (2.36)$$

$$r = (q\mu_p N_B W)^{-1} \quad (2.37)$$

$$\psi_c \approx 0.7 \text{ volt}$$

2..5.2 Bipolar transistor action of MOSFET.

The region between the source and drain can act like the base of a bipolar npn transistor, with the source acting as the emitter and the drain as the collector. Now if the substrate current produces a voltage drop in the substrate material of the order of 0.7 V, the substrate-source pn junction will conduct significantly. Electrons can be injected from the source to the substrate, just like electrons injected from emitter to base in an npn transistor. These electrons can in turn, gain sufficient energy as they travel toward the drain to cause additional impact ionization and create new electron-hole pair. This constitutes a positive feedback mechanism.

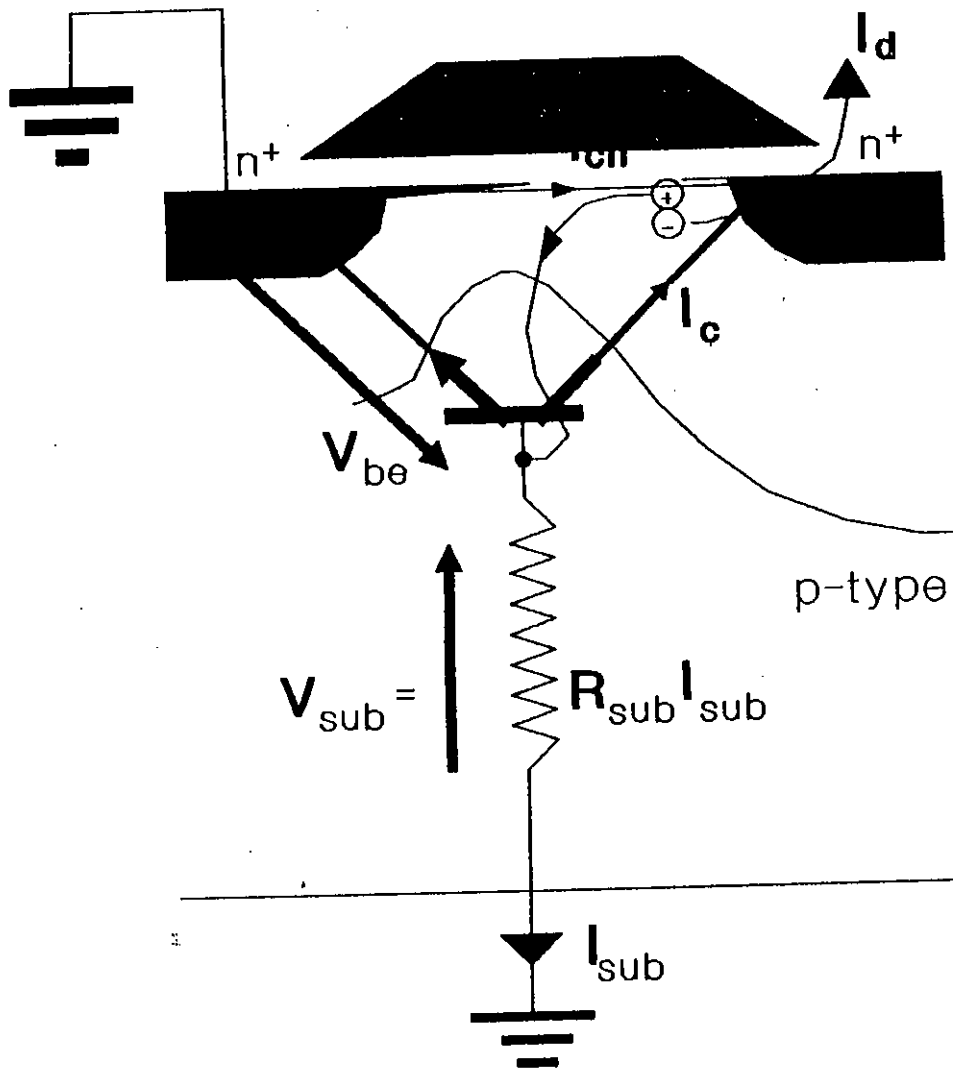


Fig.2.3 Current components due to bipolar trans action in MOSFET

The variation of base emitter junction V_{be} is [16]:

$$V_{be} = R_{sub} I_{sub} \quad ; \text{ When } V_{be} \leq 0.7 \text{ volt.} \quad (2.38)$$

$$V_{be} = \Phi_T \ln \left(1 + \frac{dN_B I_{sub}}{q \mu_p \Phi_T n_i^2 l w} \right) \quad ; \text{ When } V_{be} > 0.7 \text{ volt.}$$

(2.39)

The effect of transistor action will depend on the value of V_{be} .

2.6 CONCLUSIONS

In this chapter, hot-carrier induced substrate currents in MOSFET is presented in details. The effects of uniform electric field and nonuniform electric field on impact-ionization model have been distinguished in the analysis. The conventional drain current is derived by considering long channel MOSFET. The energy-dependent ionization model used to formulate the substrate current model has taken into account the effect of characteristic length for the electric field, energy relaxation time and the saturation velocity of electron in the pinch-off region. Finally a substrate current model is developed taking into account the facts discussed above.

CHAPTER 3

MODEL IMPLEMENTATION AND RESULTS

3.1 INTRODUCTION

The substrate current of a MOSFET depends on the drain current and ionization coefficient. Ionization coefficient is a function of drain voltage, drain saturation voltage and device parameters. The drain current is calculated by using the characteristics of long channel MOSFET. The drain saturation voltage is also determined from a developed formula. The impact ionization parameters are found from the new non-local impact ionization model. In the model, it is found that the parameters are the function of device dimensions. By using the model presented in chapter 2, the substrate current with the varying V_{GB} can be obtained for a particular V_{DB} . To know the substrate current, corresponding drain current I_D , drain saturation voltage $V_{D,SAT}$ can be calculated with the help of relevant equation derived in chapter two.

A computer program is developed to study the different characteristics of the MOSFET. The equation which are used for obtaining the characteristics are based on the analytical model developed in chapter 2. In appendix-A, we have developed an algorithm of the computer program for model simulation which is represented briefly and sequentially.

3.2 RESULTS AND DISCUSSION:

The analytical model developed in chapter 2 is used to find various characteristic of a MOSFET.

3.2.1 DRAIN CURRENT CHARACTERISTICS:

The drain current I_D vs. V_{DS} characteristic of a MOSFET taking V_{GS} as parameters is shown in Fig.- 3.1. The Fig. suggests, the effect of the gate voltage is to vary the conductance of the induced channel for low drain-to-source voltage. For a given value of V_{GS} there will be some drain voltage V_{DS} for which the current becomes saturated, after which it remains essentially constant. For a fixed drain voltage V_{DS} , if V_{GS} is increased then the pinch-off point moves toward the drain end and saturation voltage $V_{D,SAT}$ will increase. Fig. 3.2 shows the variation of drain current with gate voltage for a constant value of V_{DS} .

3.2.2 LOCAL-FIELD MODEL:

In the model, the impact ionization rate is determined directly from the field in the direction of current flow using equation (2.16) . Here A_0 and B_0 are constants and E is the uniform field. In the model, the rapid spatial varying electric

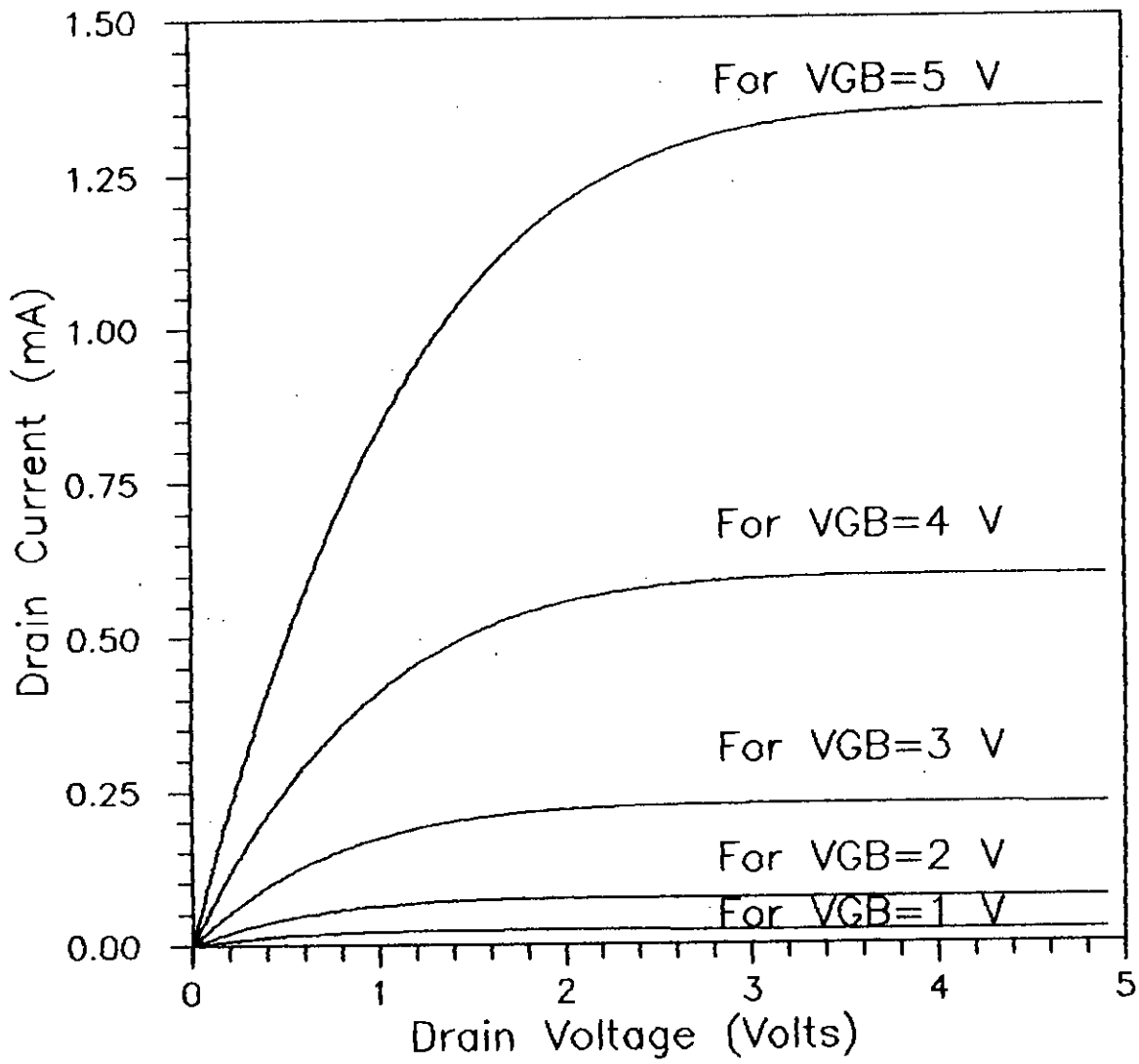


Fig. 3.1. Drain Current vs. Drain Voltage Characteristics

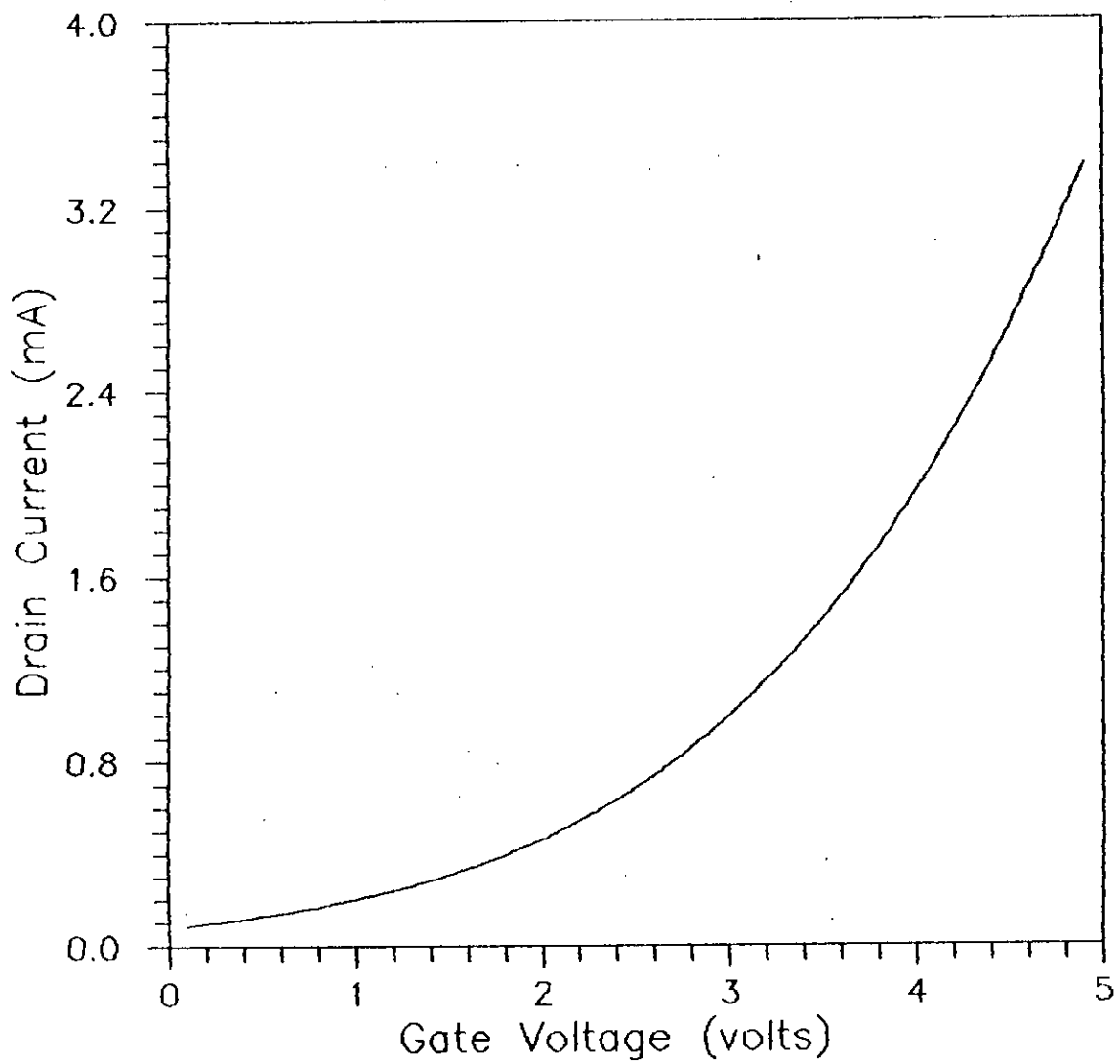


Fig. 3.2. Drain Current vs. Gate Voltage Characteristic
(For Drain Voltage=5.0 V)

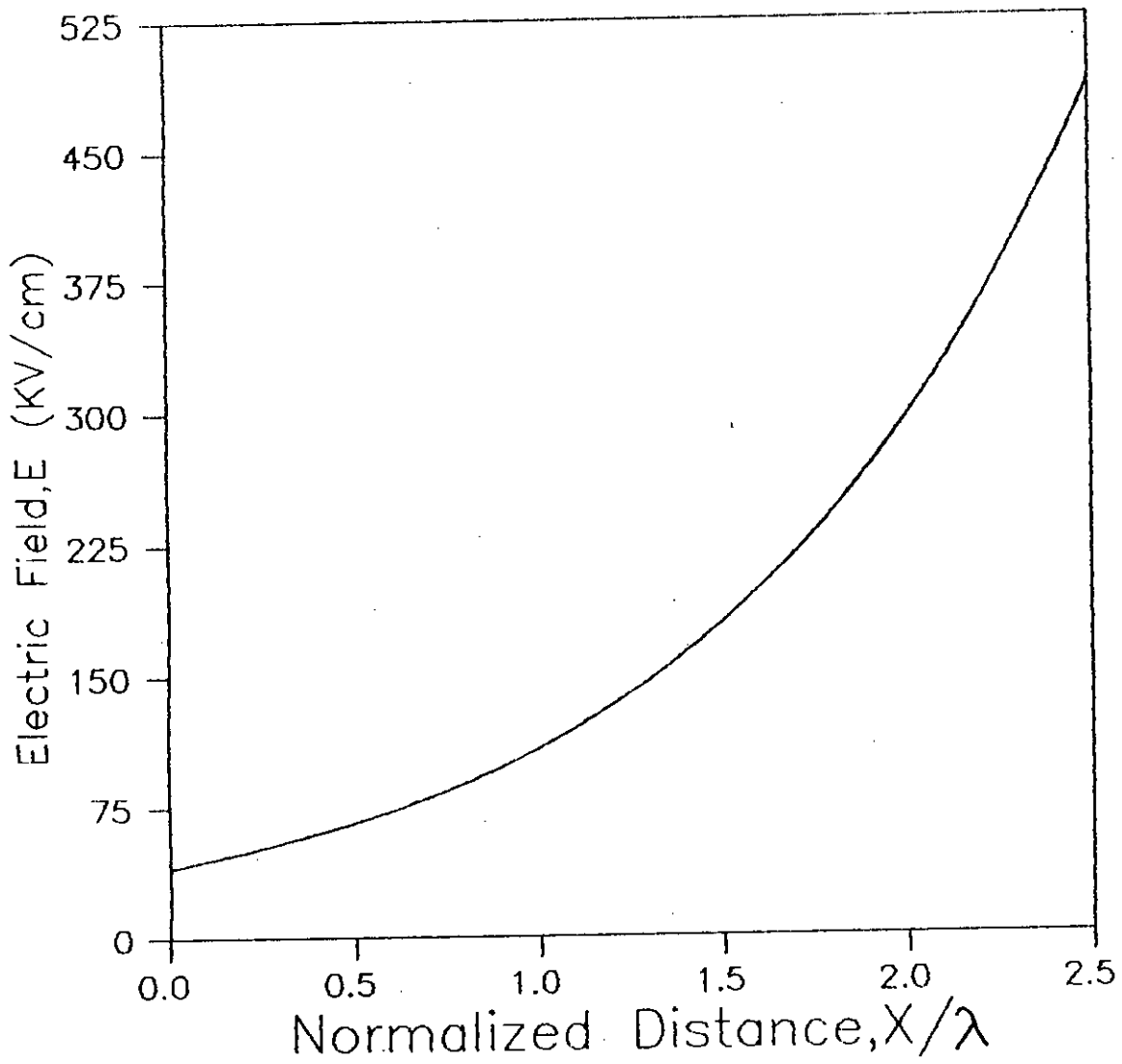


Fig. 3.3. Electric field vs. Distance normalized by the characteristic length, λ

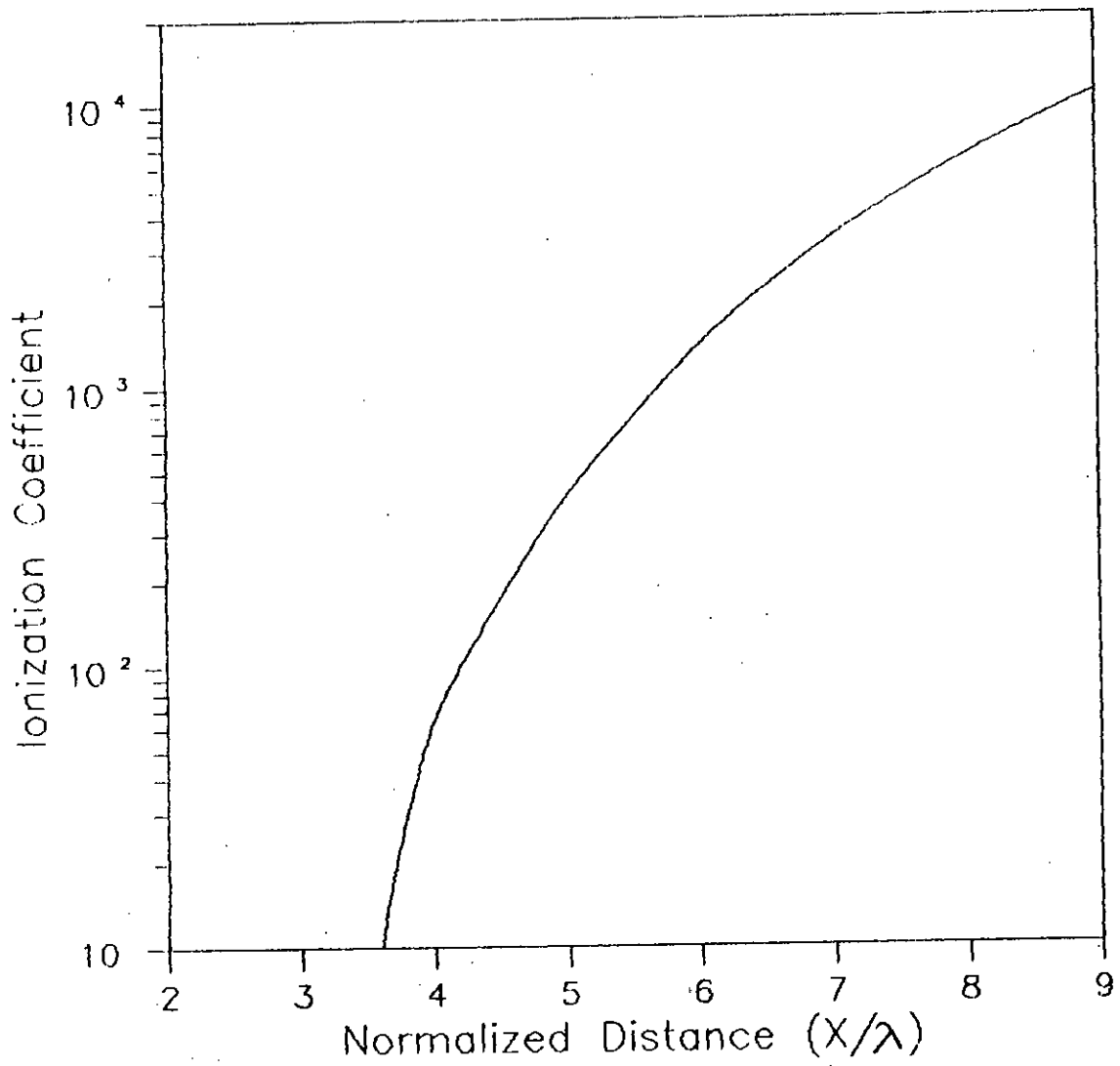


Fig. 3.4 Ionization Coefficient vs. Normalized Distance

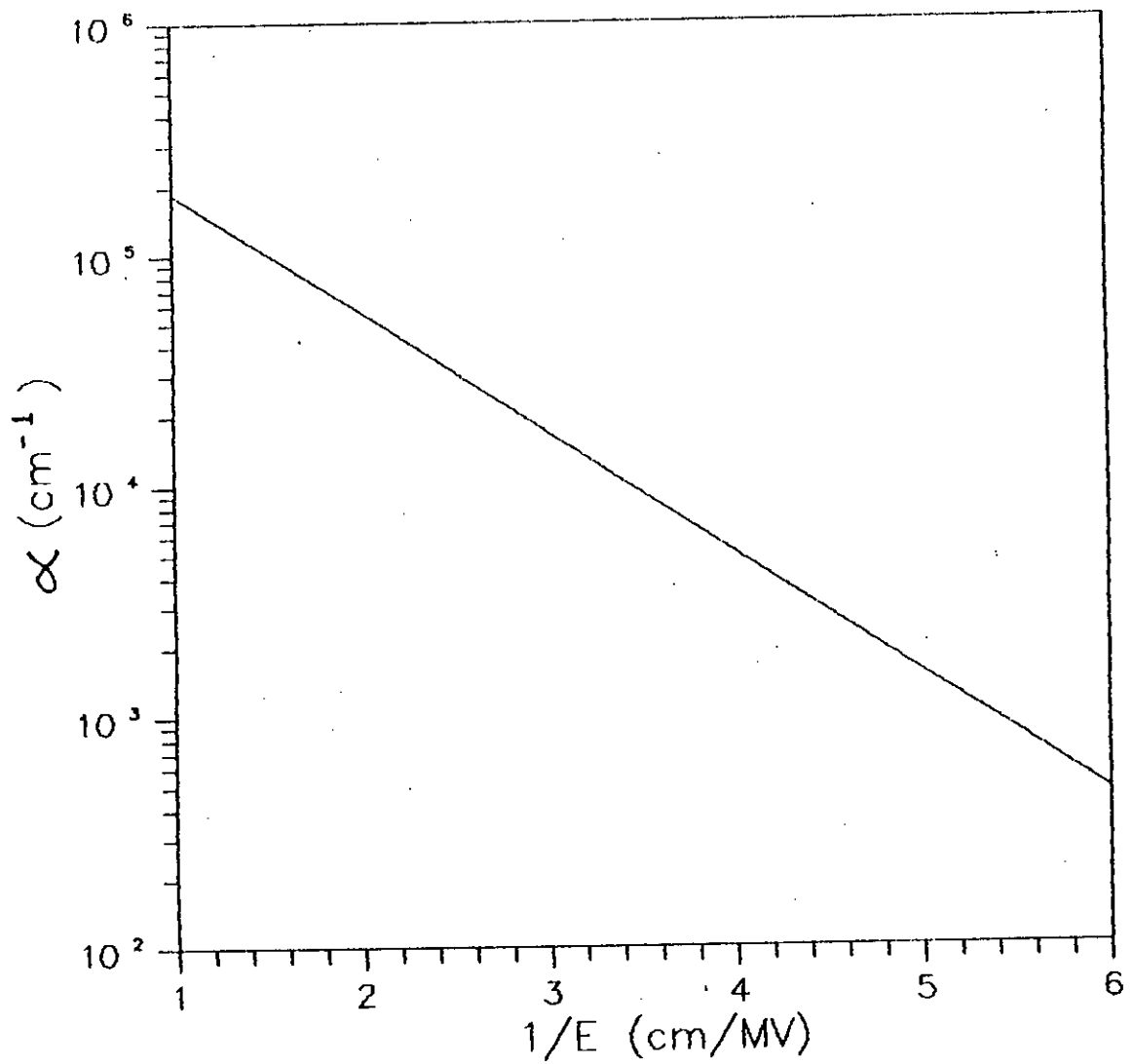


Fig. 3.5 . Impact ionization coefficient of electrons as a function of constant local field

field is used in equation (2.16) to find the model. Here, A_0 and B_0 are taken as constant value in the spatial varying electric field which depends on device dimensions.

It is seen that the model greatly overestimate the substrate current because they do not accurately model the impact ionization process in the presence of the rapidly varying fields. In the device, the experimental substrate current curves are extracted at room temperature. The model is developed with the default impact ionization coefficient. It should be noted that these co-efficient have been fitted in order to agree with the substrate current characteristics over drain biases for a single device. When the resulting equation is applied to other devices with a similar technology but different dimensions, the agreement deteriorates.

Figure-3.3 shows the variation of electric field with distance. Here, distance is measured from pinch-off point. The distance is normalized by the characteristic length λ . In figure-3.4, the impact ionization co-efficient of electrons vs. x/λ is plotted and in figure-3.5, the plot of α vs. $1/E$ is shown. The slope of the line is B_0 .

3.2.3 NON-LOCAL IMPACT IONIZATION MODEL:

In the model, the fitting parameter B is adjusted with the device dimensions. A relationship between B and λ is determined in equation (2.30). Here, the Chynoweth's law of impact ionization co-efficient in uniform field [9] shown in equation (2.16) is firstly expressed as equation (2.28), in where the impact ionization co-efficient is expressed as function of the average energy. Then, the impact ionization for varying average energy as the result of varying electric field is determined; in where the parameter is adjusted to a new value.

Figure (3.6) shows the plot of $\log \alpha$ Vs. $1/E$; the slope of the plot indicates the parameter B . It is seen that the parameter B is a function of λ . Here, it is observed that the slope of the lines increases if λ is decreased. Using the new value of $B(\lambda)$, the plot of parameter B vs. $1/\lambda$ is shown in fig. 3.7. Using the modified value of B , the developed substrate current model is better adjusted to the experimental data as compared to local field model.

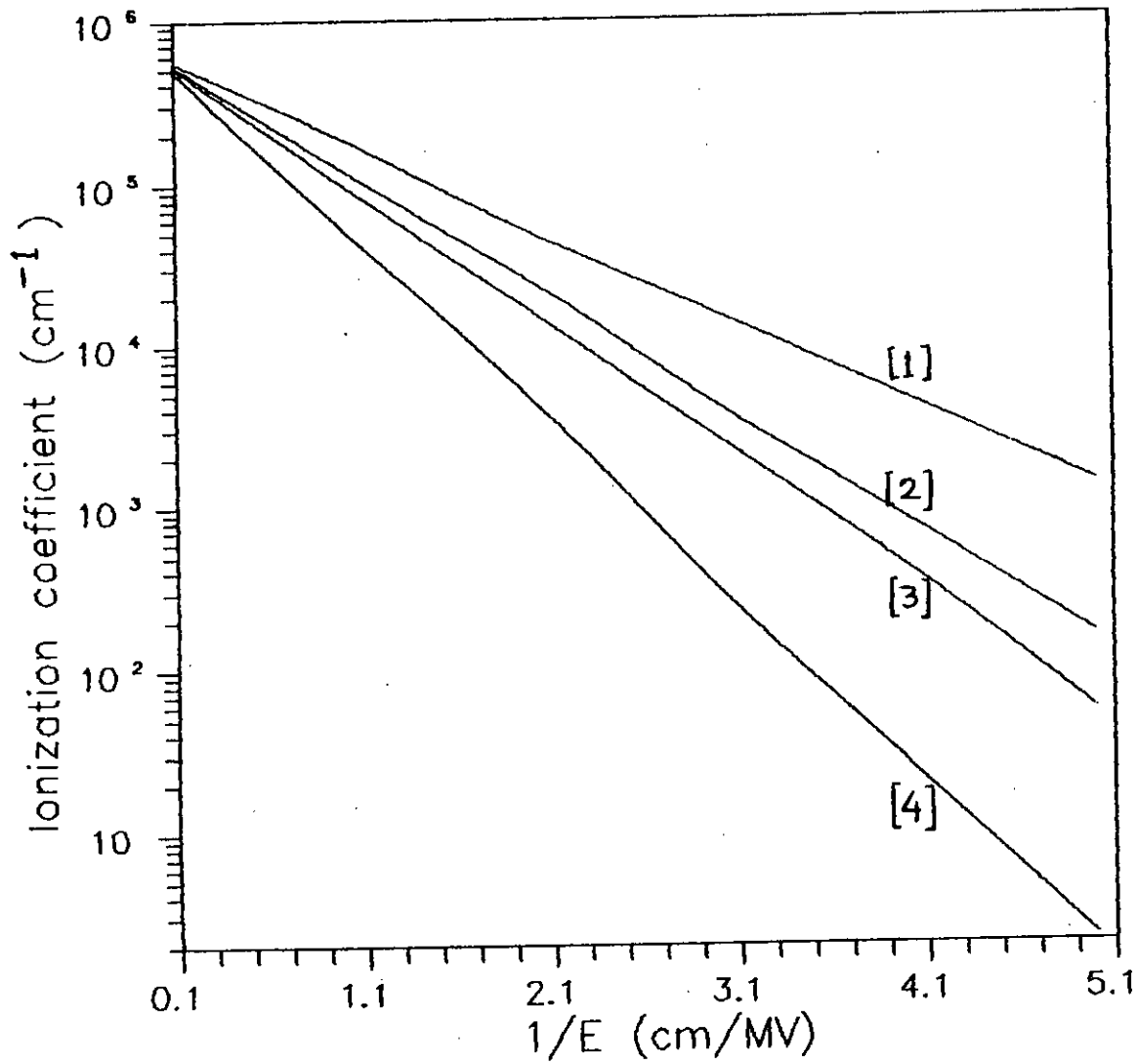


Fig. 3.6 Ionization coefficient vs. Inverse of Electric field

- 1 : Uniform field
- 2 : $\lambda = 0.3 \text{ } \mu\text{m}$
- 3 : $\lambda = 0.2 \text{ } \mu\text{m}$
- 4 : $\lambda = 0.1 \text{ } \mu\text{m}$

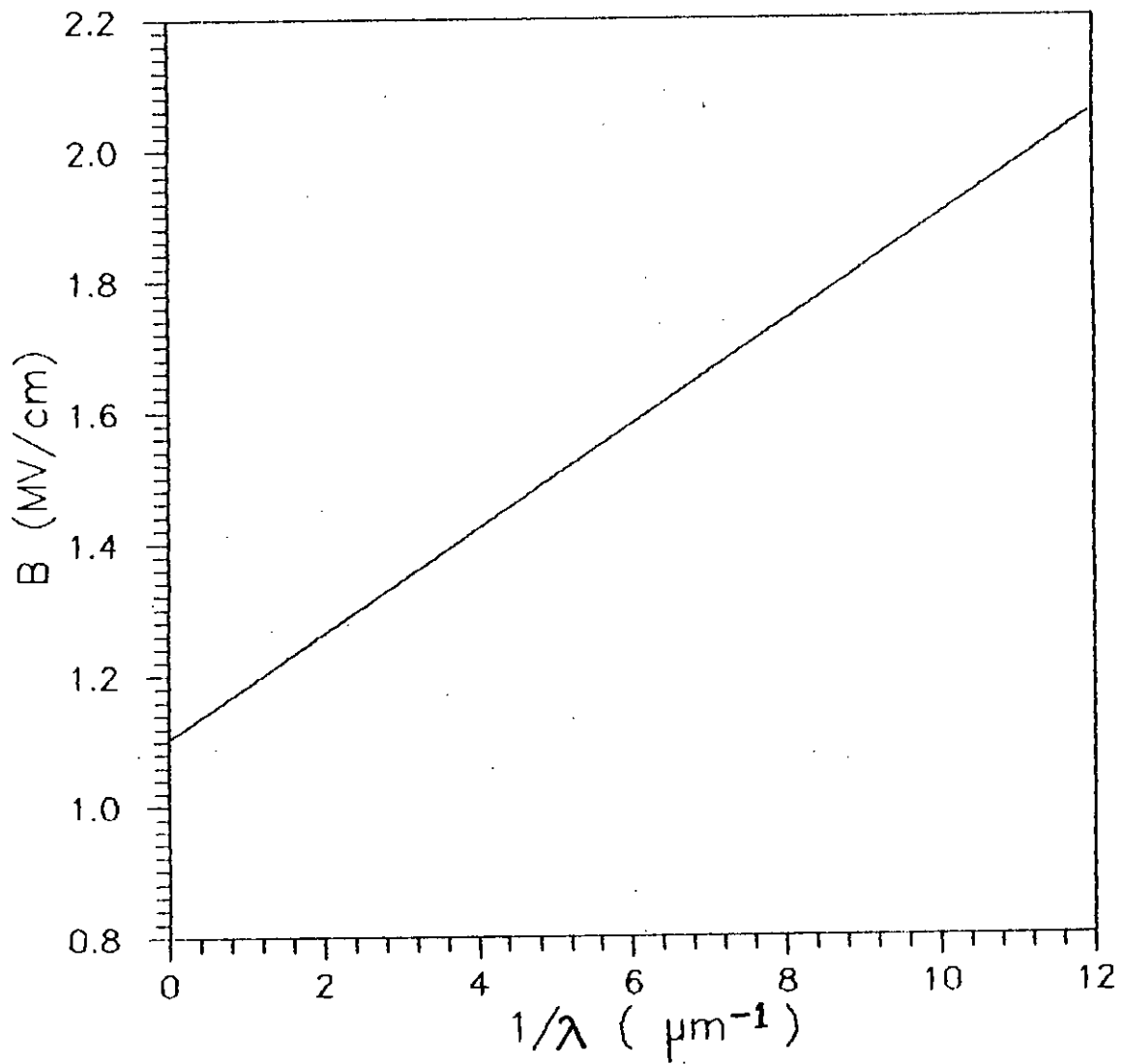


Fig. 3.7. Parameter B vs. The inverse of characteristic length, $1/\lambda$

3.2.4 SUBSTRATE CURRENT MODEL:

The variation of substrate current I_{SUB} with V_{GS} for two different values of V_{DS} is shown in fig. (3.8) and fig. (3.9). The substrate current, I_{SUB} increases first with V_{GS} reaches a maximum, then decreases[17]. We show that substrate current is proportional to both the drain current, I_D and ionization co-efficient, α . For a given V_{DS} , as V_{GS} increases, both I_D and $V_{D, SAT}$ increase. When $V_{D, SAT}$ increases the lateral field $(V_D - V_{D, SAT})/\Delta L$ decreases, causing a reduction of α . thus we have two conflicting factors. The initial increase of I_{SUB} is caused with V_{GS} , and at larger V_{GS} , the decrease of I_{SUB} is due to decrease of α . Maximum I_{SUB} occurs where the two factors balance.

In fig. (3.8) and fig. (3.9), both the measured and calculated substrate current are shown. The simulation results with non-local impact ionization model agrees quite well with the measured data[14]. But, the calculated result based on local-field model significantly differs from the measured data. Moreover, relative error become large as the drain voltage or electric field decreases in case of local field. Since the substrate current is comparable with the drain current in the subthreshold region, the assumption of very low substrate current with respect to drain current is not very appropriate as the case of lower drain voltage. It is seen that fig.(3.8) fits

better to the practical data as compared to fig. (3.9). This may be due to the inaccuracy in the assumed values of various device parameters e.g. effective mean free path for electrons.

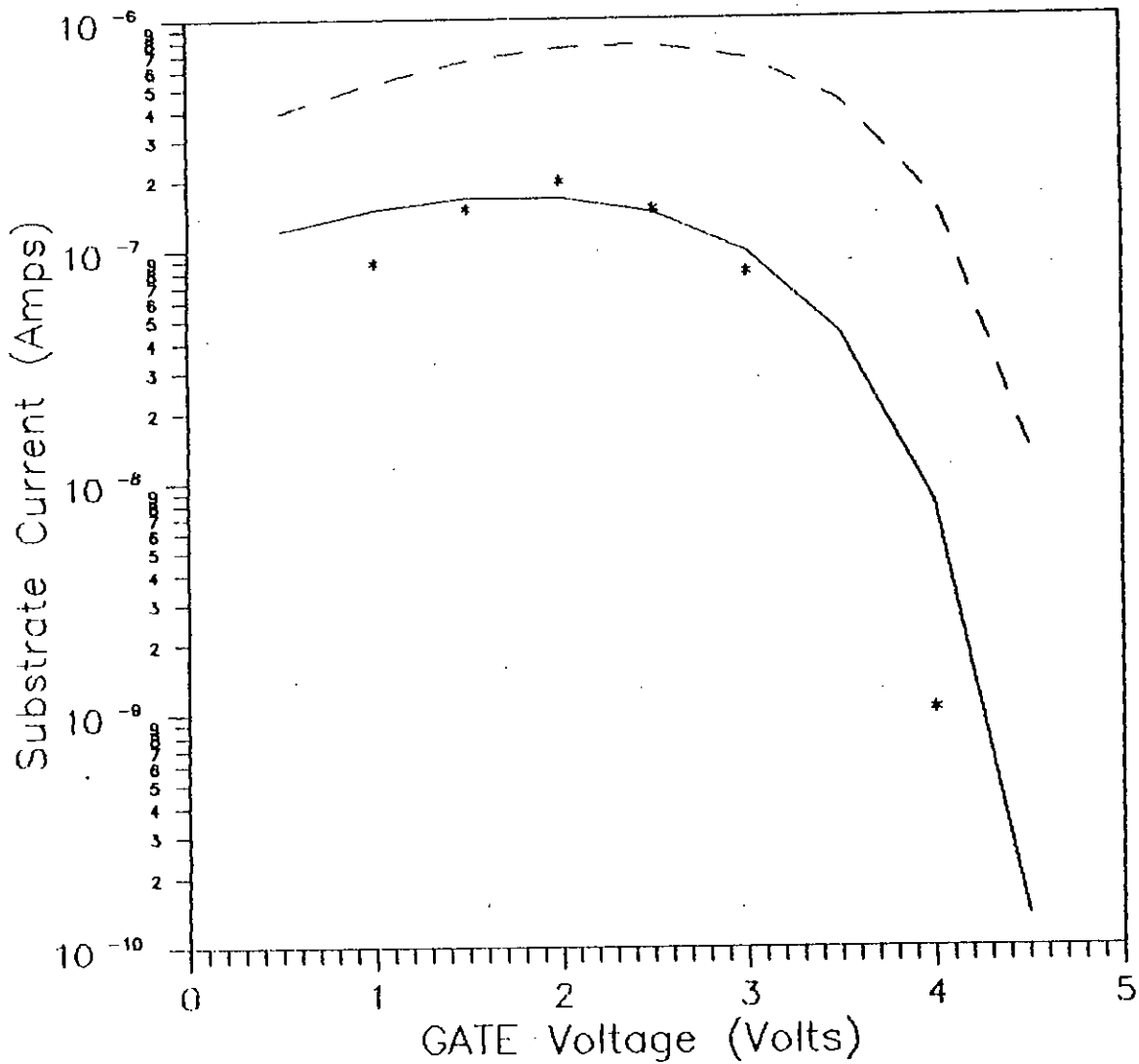


Fig.3.8 Substrate Current vs. Gate Voltage Taking Drain Voltage = 5 Volts

* * * : For Practical Data
 - - - : For Local Field Model[5]
 ——— : For nonlocal Field Model

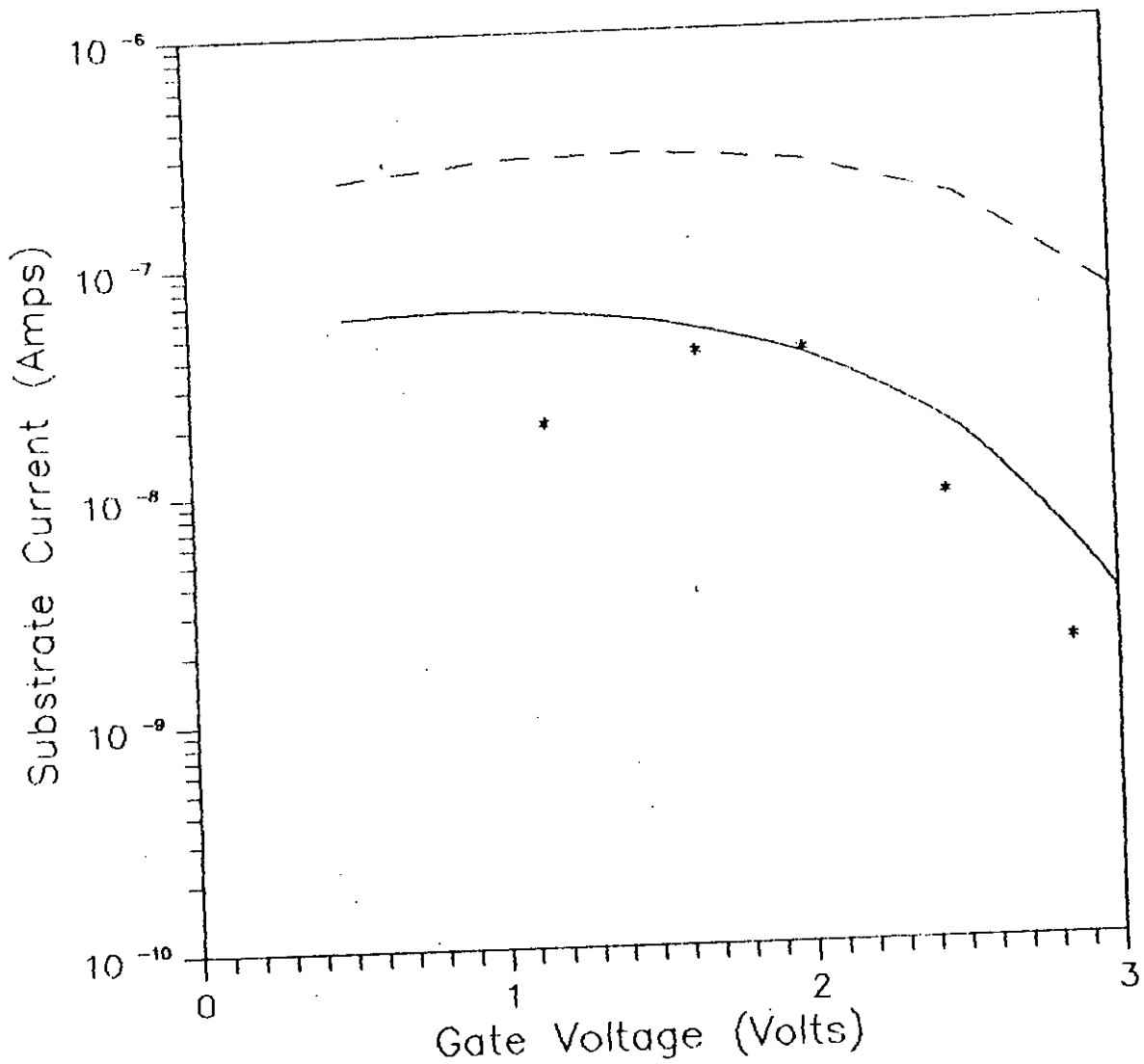


Fig. 3.9). Substrate Current vs. Gate Voltage Taking
 Drain Voltage = 4.0 Volts
 * * * :For Practical Data
 - - - :For Local Field Model[5]
 ——— :For nonlocal Field Model

3.2.5 Depletion width and the base emitter voltage

Fig. 3.10 shows the variation of depletion width w with substrate current I_{sub} . The depletion width w decreases with the increase of substrate current which can be explained by equation (2.35). The depletion width w is a function of I_{sub} for a fixed w and decreases with the increase of I_{sub} due to the decrease of the second term of the square root portion of equation (2.35). The increase in substrate current corresponds to a increase in the number of holes which causes a reduction in depletion width w .

Fig. 3.11 shows the dependence of base emitter voltage V_{be} of the MOSFET on I_{sub} . In the present device, the V_{be} is less than 0.7 V; so that it does not turn on the transistor action.

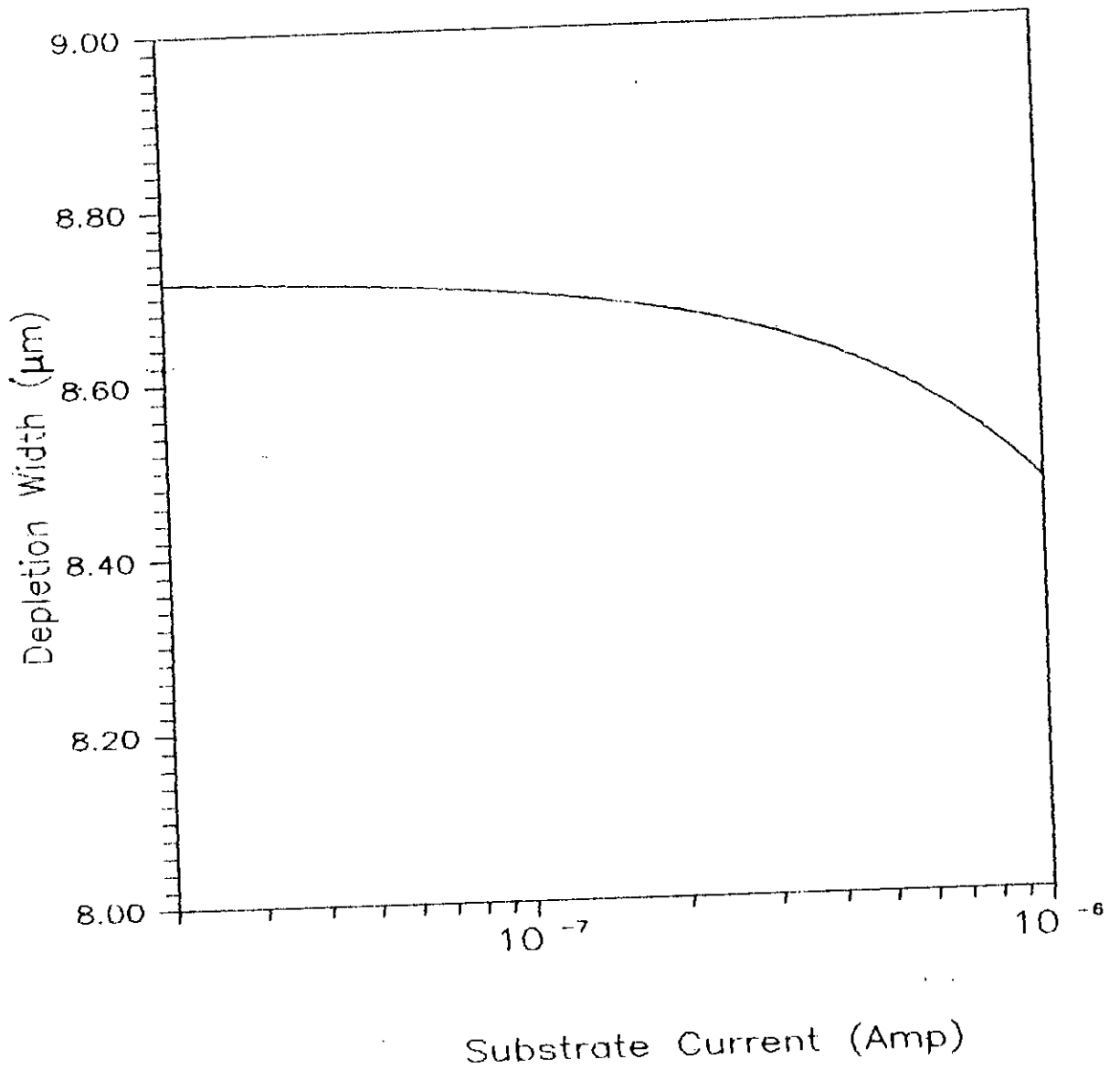


Fig.3.10 Effect of substrate current on depletion width

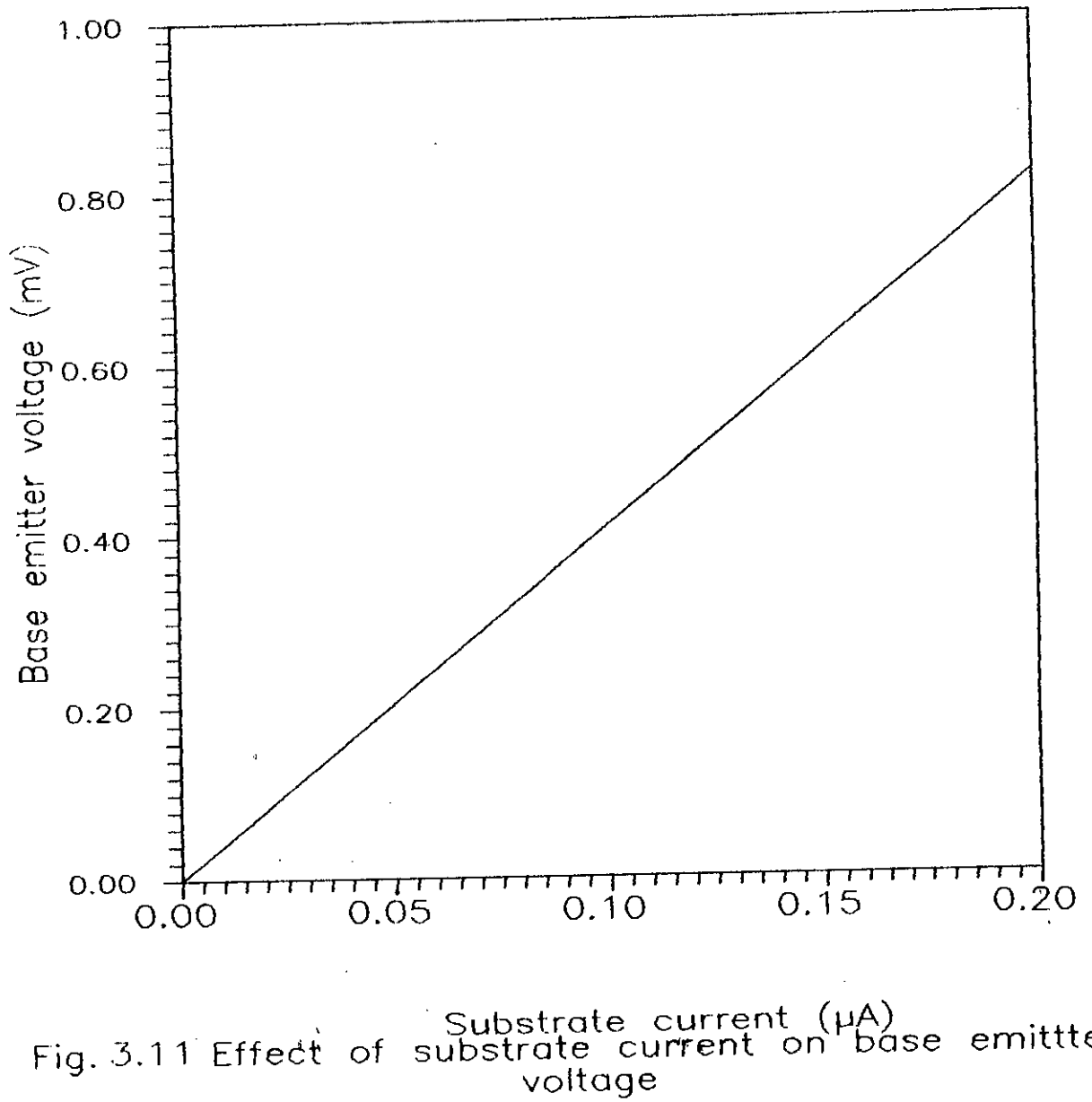


Fig. 3.11 Effect of substrate current on base emitter voltage

3.3 CONCLUSIONS:

The substrate current characteristics are studied by using the model described in chapter-2. A computer program is developed based on the algorithm illustrated in appendix-A. The simulated results of substrate currents using the proposed model show a reasonable agreement with the experimental data and give a better performance than the local field model. The local field model uses the default impact ionization coefficients which overestimates the substrate current. The developed non-local impact ionization model modifies the fitting parameter of Chynoweth's law and thus give a new substrate current model of better performance.

90718

CHAPTER 4

CONCLUSIONS AND SUGGESTIONS

4.1 CONCLUSIONS:

In this work, an analytical model of substrate current in MOSFET is presented. Simple and accurate device modeling is required to predict the performance of the device. But accurate modeling of a device is very difficult and complex. There is always a trade-off between accuracy and complexity. Apparent disagreements between experimental and calculated data can be explained in the following way:

Since the substrate current is comparable with the drain current in the subthreshold region, the assumption of very low substrate current with respect to drain current is not very appropriate. When the substrate current begins to be an appreciable fraction of the drain current, then a two-carrier solution of the energy transport equations is more valid than the single carrier solution.

Moreover, in the determination of drain current, short channel effects are not included. So the calculated drain current is not an exact estimation of the drain current in case of short channel MOSFET.

The proposed non-local impact ionization co-efficient is applicable for the drain region of n-channel MOSFET's where electric field increases exponentially. Considering the above effects, the new substrate current model is derived from the developed impact ionization model. Finally, the developed model is compared with some published experimental data. It is observed from the comparison that the non-local impact ionization model agrees better with the experimental data. So it can be concluded that the proposed model for substrate current explains the experimental data much better than the existing local field model.

4.2 SUGGESTIONS

In this work, the additional effects in drain current due to shot-channel MOSFET's are not incorporated. Also the effect of substrate current on drain current in the subthreshold region is not considered in calculating drain currents. The drain current is determined by one dimensional analysis. However the breakdown physics in short channel MOSFET along with various short channel effects are three dimensional which is extremely difficult to approach analytically. The proposed model can further be improved by incorporating all these effects.

APPENDIX-A

The substrate current of a MOSFET can calculate from drain current, drain voltage, drain saturation voltage, characteristic length for the electric field etc. The relevant equations required to get these component are derived in chapter 2. The drain current can calculate from equation (2.1). The drain saturation voltage can be determined from equation (2.13). The parameter B is evaluated from equation (2.30). The flow chart of the computational method used to obtain the I_{SUB} versus V_{GB} characteristic is shown in (Fig. 4.1) . The steps of the total algorithm are shown below:

1. Start the program.
2. Read the necessary parameters like drain bulk voltage V_{DB} , source bulk voltage V_{SB} , field at saturation E_{SAT} , junction depth X_j , oxide thickness t_{ox} , doping concentration of substrate N_A , channel length L and channel width etc .
3. Take gate-to-bulk voltage V_{GB} to 0.5 volts.

4. Determine the surface potential at pinch-off point by using subprogram CALC.
5. Determine also the surface potential at drain end by using the subprogram CALC.
6. Calculate the drain current , I_D by calculating the drift current and diffusion current.
7. Calculate the drain saturation voltage, $V_{D,SAT}$ by using the analytical expression
8. Using the drain current I_D , drain voltage V_D , drain saturation voltage $V_{D,SAT}$, find the substrate current at the corresponding gate-to-bulk voltage, V_{GB} .
9. Print V_{GB} and corresponding I_{SUB} .
10. Increase the gate-to-bulk voltage by 0.5 volts if gate voltage is less than the ending limit, repeat from step-4.
11. Stop.

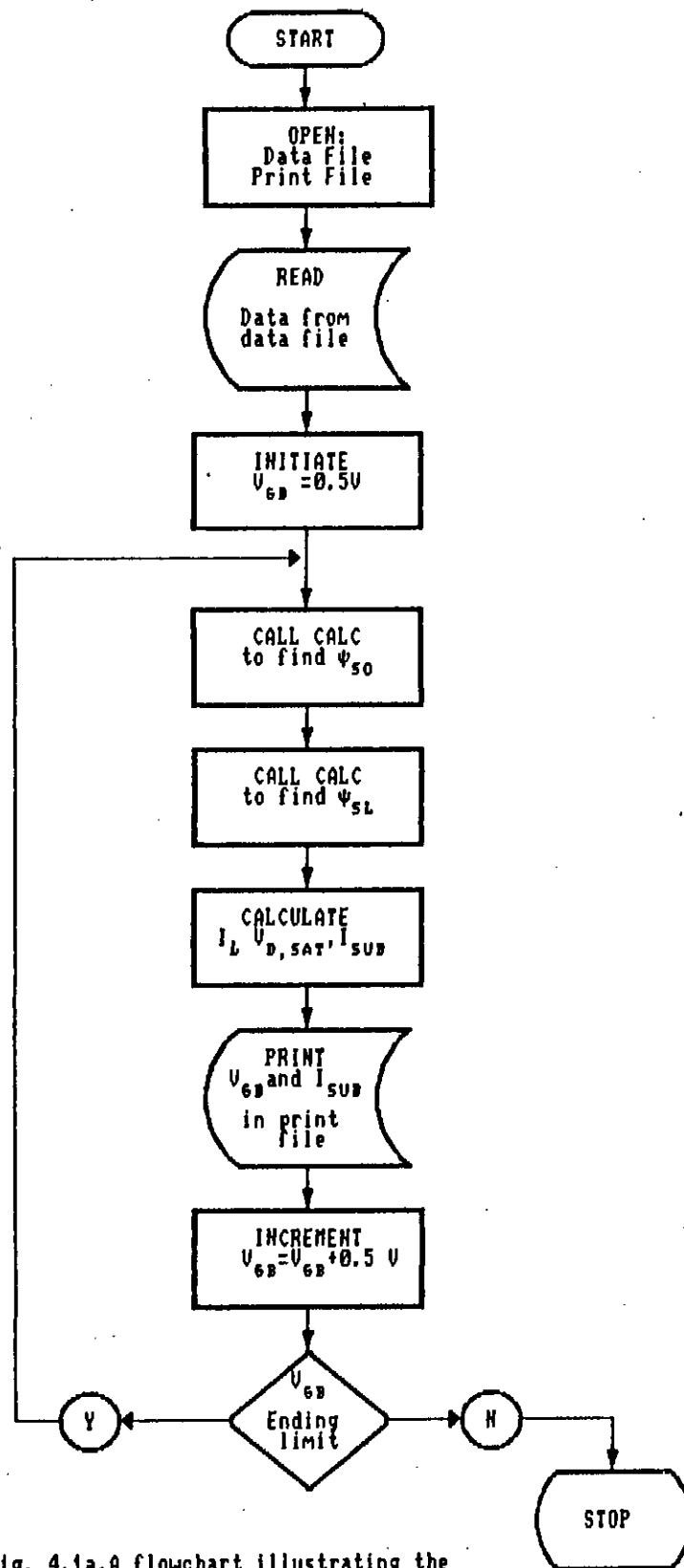


Fig. 4.1a. A flowchart illustrating the procedure of finding substrate current characteristics.

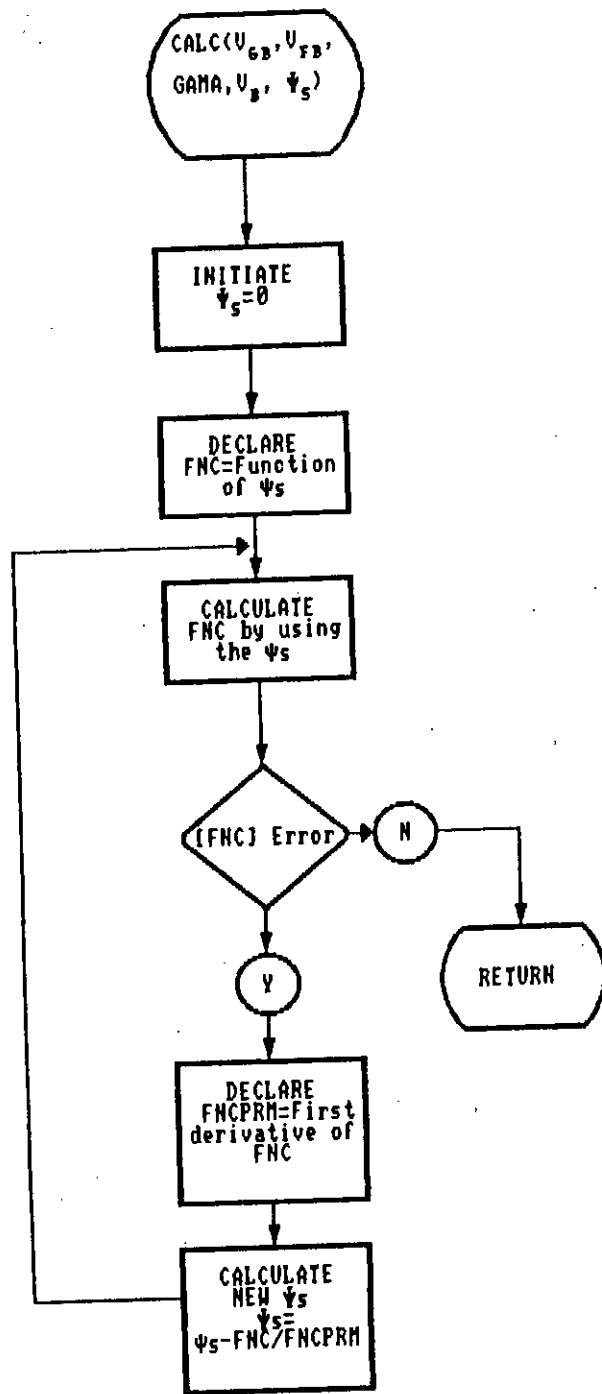


Fig.4.1b. A flow of a subprogram illustrating the procedure of finding surface potential.

The algorithm of determining the surface potential used to find drain current is shown below. It is used as a subprogram of the main program unit.

1. Assume a value of surface potential , ψ_s .
2. Declare the transcendal equation of ψ_s as a function , FNC. Find FNC by using the value of ψ_s .
3. If FNC is less than or equal to a tolerable error, go to step-7.
4. Declare the first derivative of FNC as FNCPRM. Determine FNCPRM by using the value of ψ_s .
5. Determine a new value of ψ_s from the relation of
$$\psi_s = \psi_s - \text{FNC}/\text{FNCPRM}$$
6. Repeat from step 2.
7. Repeat to the main program.

Using equation (2.5)-(2.7), the drain current is calculated at a particular gate-bulk voltage V_{GB} for a fixed drain-bulk voltage V_{DB} . In the computation, the surface potential at the pinch-off point and the surface potential at the drain end is calculated from equation (2.8) - (2.9) by applying Newton Raphson method.

The parameter of impact ionization co-efficient $B(\lambda)$ is calculated from the developed equation (2.30). The drain saturation voltage $V_{D,SAT}$ is determined from the developed equation (2.15). Using these values, the substrate currents for various gate-bulk voltage for a fixed drain-bulk voltage is found by using equation (2.34). The calculation is started from $V_{GB} = 0.5$ volts. It is repeated by increasing V_{GB} in 0.5 volts in each step; when $V_{GB} >$ ending limit, the calculation is stopped.

Besides the main program four separate programs have been developed to find I_D as a function of V_{DS} , I_D as a function of V_{GS} , ionization coefficient as a function of inverse electric field, and parameter B as a function of $1/\lambda$. Newton-Raphson method is used as a subprogram along the main program to extract the value of surface potential which is necessary to find the drain current.

APPENDIX-B

RELATIONSHIP BETWEEN IONIZATION COEFFICIENT AND ELECTRIC FIELD.

The charge multiplication, M , produced by carrier injection into a p-n junction can measure as a function of the bias, V for the two different grown junction , Let, junction A is n type and junction B is p type. Considering the multiplication initiated by hole injection, we have [20]

$$1 - \frac{1}{M} = \int_0^w \alpha(E) \exp\left\{ \int_0^x [\alpha(E) - \beta(E)] dx' \right\} dx \quad (1)$$

where, α and β are the ionization rate for electrons and holes respectively. A similar expression of equation (1) results for the case of electron injection if α and β are interchanged.

$$1 - \frac{1}{M} = \int_0^w \beta(E) \exp\left\{ - \int_0^x [\beta(E) - \alpha(E)] dx' \right\} dx \quad (1.2)$$

The solution of these two simultaneous equations in α and β can be found by considering an uniform field over an appropriate effective width.

The results of these calculations show that, within the limit of experimental error, plotting the logarithm of the ionization rate against the reciprocal of the electric field strength results and probably, for electrons also. So the relationship between α and E can be expressed as,

$$\alpha = A \exp(-B / E)$$

Where, A and B are constants.

REFERENCES

- [1] E.S. Yang, "Microelectronic Devices," Mc-Graw-Hill Book Company, 1988, pp-260, 266.
- [2] D.P. Kennedy and A. Philips, "Source-drain breakdown in an insulated gate field transistor," IEDM Tech. Dig., pp. 160, 1973.
- [3] T. Toyable, K. Yamaguchi, and S. Asai, "A two-dimensional avalanche breakdown model of submicron MOSFET's" IEDM Tech. Dig. pp. 432, 1978.
- [4] F. Hsu, P. Ko and S. Tam, "An analytical breakdown model for short channel MOSFET's IEEE Transactions on Electron Devices, Vol. ED-29, 1982, pp. 1735-1739.
- [5] V.M. Agostinelli JR., K. Hasnat, T.J. Bordelon, D.B. Lemersal JR., and C.M. Maziar, "Sensitivity issues in modeling the substrate current for submicron N- and P- channel MOSFET." Solid State electronics vol.37, No.-9, pp1627-1632, 1994.

[6] R. K. Cook and J. Frey, "Two-dimensional numerical simulation of energy transport effects in Si and GaAs MESFET's, IEEE Transactions on Electron Devices, Vol. ED-29, No.6, June 1982.

[7] N. Goldman and J. Frey, "Efficient and accurate use of the energy transport method in device simulation, "IEEE Trans. Electron Devices, Vol. 35, pp. 1524-1529, 1988.

[8] C.G. Hwang, R.W. Dutton. " Substrate Current Model for Submicrometer MOSFET's based on mean free path analysis." IEEE Trans. on Electron devices, vol. 36, No.7, July 1989.

[9] Chynoweth, A.G., " Ionization rates for electrons and holes in silicon, "Physics Rev. Vol. 109, pp. 1537-1540, 1958.

[10] R. V. Overstraeten, H.D. Man, "Measurement of the ionization rates in diffused silicon p-n junctions, "Solid-state Electron, Vol. 13, pp. 583-608, 1970.

[11] A. Sheutz, S.selberherr and H.W. Potzi, " A two dimensional model of the avalanche effect in MOS transistors ", Solid State Electronics, vol.25, No3, pp 177-183, 1982

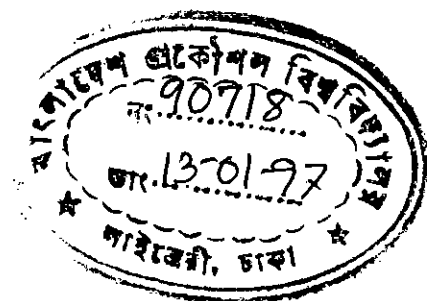
[12] T.C. Ong, P.K.Ko., C.HE, " Hot Carrier Current modeling and device degradation in surface channel p-MOSFET's, "IEEE transactions on Electron Devices, vol.37, July 1990.

[13] J.H. Huang , G.B. Zhang, Z.H. Liu, "Temperature dependent of MOSFET substrate current" , IEEE Electron device letters , vol. 14 No. 5 , May 1993.

[14] G.S. Huang and C.Y. Wu," An analytic saturation model for drain and substrate currents of conventional and LDD MOSFET's ", IEEE Trans. on Electron Devices, Vol. 37, No.7, July 1990 .

[15]P.K.Ko,"Advanced MOS Devices," John Willely, 1988, Page 24-34.

[16] Md. Tanvir Quddus, " Analytical modeling of breakdown in short channel MOSFET's" master's thesis, October 1993, BUET, Dhaka.



[17] S.M.Sze, "Physics of Semiconductor Devices," John Willey, 1969, pp. 480-483.